Histological, metabolomic, and transcriptomic differences in fir trees from a peri-urban forest under chronic ozone exposure

Juan P. Jaramillo-Correa[1], Verónica Reyes-Galindo[2], Svetlana Shishkova[3], Estela Sandoval-Zapotitla[4], Cesar M. Flores-Ortiz[5], Daniel Piñero[6], Lewis Spurgin[7], Claudia Martin[7], Ricardo Torres-Jardón[8], Claudio Zamora-Callejas[9], and Alicia Mastretta-Yanes[10]

[1]Institute of Ecology, Universidad Nacional Autónoma de México
[2]Universidad Nacional Autónoma de México Instituto de Ecología
[3]Universidad Nacional Autónoma de México Instituto de Biotecnología
[4]Universidad Nacional Autónoma de México Instituto de Biología
[5]Universidad Nacional Autonoma de Mexico
[6]Universidad Nacional Autónoma de México
[7]University of East Anglia
[8]Universidad Nacional Autónoma de Mexico, Instituto de Ciencias de la Atmósfera y Cambio Climático
[9]Bienes Comunales Santa Rosa Xochiac
[10]CONACYT Research Fellow assigned to CONABIO

May 23, 2024

Abstract

Urbanization modifies ecosystem conditions and evolutionary processes. This includes air pollution, mostly as tropospheric ozone (O3), which contributes to the decline of urban and peri-urban forests. A notable case are fir(Abies religiosa) forests in the peripheral mountains southwest of Mexico City, which have been severely affected by O3 pollution since the 1970s. Interestingly, some young individuals exhibiting minimal O3—related damage have been observed within a zone of significant O3 exposure. Using this setting as a natural experiment, we compared asymptomatic and symptomatic individuals of similar age ([?]15 years old; n = 10) using histological, metabolomic and transcriptomic approaches. Plants were sampled during days of high (170 ppb) and moderate (87 ppb) O3 concentration. Given that there have been reforestation efforts in the region, with plants from different source populations, we first confirmed that all analysed individuals clustered within the local genetic group when compared to a species-wide panel (Admixture analysis with ˜1.5K SNPs). We observed thicker epidermis and more collapsed cells in the palisade parenchyma of needles from symptomatic individuals than from their asymptomatic counterparts, with differences increasing with needle age. Furthermore, symptomatic individuals exhibited lower concentrations of various terpenes (ß-pinene, ß-caryophylene oxide, α-caryophylene and ß-α-cubebene) than asymptomatic trees, as evidenced through GC-MS. Finally, transcriptomic analyses revealed differential expression for thirteen genes related to carbohydrate metabolism, plant defense, and gene regulation. Our results indicate a rapid and contrasting phenotypic response among trees, likely influenced by standing genetic variation and/or plastic mechanisms. They open the door to future evolutionary studies for understanding how O3 tolerance develops in urban environments, and how this knowledge could contribute to forest restoration.

Histological, metabolomic, and transcriptomic differences in fir trees from a peri-urban forest under chronic ozone exposure

Verónica Reyes-Galindo[1,2*], Juan Pablo Jaramillo-Correa[1], Svetlana Shishkova[3], Estela Sandoval-Zapotitla[4], Cesár Mateo Flores-Ortiz[5], Daniel Piñero[1], Lewis G. Spurgin[6], Claudia A. Martin[6], Ricardo Torres-Jardón[7],Claudio Zamora-Callejas[8], Alicia Mastretta-Yanes[9,10*]

[1] Department of Evolutionary Ecology, Institute of Ecology, Universidad Nacional Autónoma de México, AP 70-275 Mexico City, CDMX 04510, México

[2] Programa de Maestría en Ciencias Biológicas, Universidad Nacional Autónoma de México, Mexico City, CDMX, México

[3] Departamento de Instituto de Biotecnología, Universidad Nacional Autónoma de México, Cuernavaca, Morelos 62210, México

[4] Jardín Botánico, Instituto de Biología, Universidad Nacional Autónoma de México, AP 70-640 Mexico City, CDMX 04510, México

[5] Unidad de Biotecnología y Prototipos, Facultad de Estudios Superiores Iztacala, Universidad Nacional Autónoma de México, Estado de México, Tlalnepantla 54090, México

[6] University East of Anglia, School of Biological Sciences, Norwich, UK

[7] Centro de Ciencias de la Atmósfera, Universidad Nacional Autónoma de México, Mexico City, CDMX 04510, México

[8] Bienes Comunales Santa Rosa Xochiac, Mexico City, CDMX, México

[9] Comisión Nacional para el Conocimiento y Uso de la Biodiversidad. Mexico City, CDMX 14010, México

[10] Consejo Nacional de Ciencia y Tecnología. Mexico City, CDMX, 03940, México.

*Corresponding authors:
Veronica Reyes-Galindo: veronica.rg.pb@gmail.com
Alicia Mastretta-Yanes: amastretta@conabio.gob.mx
Juan Pablo Jaramillo-Correa: jaramillo@ecologia.unam.mx
Key words: *Abies religiosa*, ozone pollution, transcriptomic, terpenes, natural conditions.

Abstract

Urbanization modifies ecosystem conditions and evolutionary processes. This includes air pollution, mostly as tropospheric ozone (O_3), which contributes to the decline of urban and peri-urban forests. A notable case are fir(*Abies religiosa*) forests in the peripheral mountains southwest of Mexico City, which have been severely affected by O_3 pollution since the 1970s. Interestingly, some young individuals exhibiting minimal O_3—related damage have been observed within a zone of significant O_3 exposure. Using this setting as a natural experiment, we compared asymptomatic and symptomatic individuals of similar age (≤15 years old; *n* = 10) using histological, metabolomic and transcriptomic approaches. Plants were sampled during days of high (170 ppb) and moderate (87 ppb) O_3 concentration. Given that there have been reforestation efforts in the region, with plants from different source populations, we first confirmed that all analysed individuals clustered within the local genetic group when compared to a species-wide panel (Admixture analysis with ~1.5K SNPs). We observed thicker epidermis and more collapsed cells in the palisade parenchyma of needles from symptomatic individuals than from their asymptomatic counterparts, with differences increasing with needle age. Furthermore, symptomatic individuals exhibited lower concentrations of various terpenes (ß-pinene, ß-caryophylene oxide,

α-caryophylene and ß-α-cubebene) than asymptomatic trees, as evidenced through GC-MS. Finally, transcriptomic analyses revealed differential expression for thirteen genes related to carbohydrate metabolism, plant defense, and gene regulation. Our results indicate a rapid and contrasting phenotypic response among trees, likely influenced by standing genetic variation and/or plastic mechanisms. They open the door to future evolutionary studies for understanding how O_3 tolerance develops in urban environments, and how this knowledge could contribute to forest restoration.

Introduction

Rapid urbanization has severely disturbed entire ecosystems since the beginning of the industrial age (Bai et al., 2017), raising the important questions of how species cope with human-transformed environments and which molecular, evolutionary and ecological processes are involved (Rivkin et al., 2019). It is regularly thought that for species to persist in urban areas, they must adapt rapidly (Johnson & Munshi-South, 2017). However, for adaptation to occur, selection needs to operate on heritable variation, which can determine whether a species persists or disappears from urban areas. Rapid adaptation seems particularly important for pollution tolerance, one of the strongest and most abrupt challenges that an urban species may face (Santangelo et al., 2018). This is especially challenging for long-lived species, such as forest trees, implying that adaptation must occur within a few generations or be complemented by plastic responses (Müller-Starck & Schubert, 2001). The genetic basis and plastic responses to pollution have been studied using a plethora of methods, from traditional provenance trials to genomic and transcriptomic analyses (Papadopulos et al., 2020; Whitehead et al., 2017). However, most research has been done under controlled conditions, meaning that studies in natural settings are

needed for exploring the differential phenotypic responses in putatively tolerant versus sensitive individuals, and verifying if the same genes and pathways pinpointed in controlled studies can also be detected in the field.

One of the most common and harmful urban pollutants is tropospheric ozone (O_3), which is generated by photochemical reactions that involve by-products of fossil fuel burning (Churkina et al., 2017). Ozone is toxic to plants and has caused significant damage to forest ecosystems in and around heavily polluted cities (Ashmore, 2005; Cho et al., 2011). Given the key role that urban forests perform as providers of ecosystem services, understanding how O_3 tolerance operates in trees is a pivotal step for informing conservation and reforestation programs of degraded (peri-)urban forests. This requires field studies with an urban-ecology perspective, aiming to understand how O_3 tolerance develops and operates in natural settings, where tree responses to O_3 are also expected to be more complex and entangled with other sources of stress (Nunn et al., 2006).

In plants, O_3 damage, and the molecular mechanisms underlying the response to O_3 exposure, has been studied for over 20 years, using both field and laboratory experiments with controlled conditions (Felzer et al., 2007; Hayes et al., 2020). O_3 enters the plant through the stomata and triggers the formation of different reactive oxygen species (ROS), causing metabolic stress and resulting in cellular death, as ROS travel through the apoplast (Tausz et al., 2007). Several candidate genes have been postulated to cope with O_3-mediated metabolic stress (*e.g.,* Hayes et al., 2020). However, strategies seem to differ between species and among populations within species (Baier et al., 2005; Hasan et al., 2021; Ludwików & Sadowski, 2008). For instance, differential sensitivity to ozone has been documented between poplars from more polluted and less polluted areas in the USA, according to

101 both common garden and field experiments (Berrang et al., 1991). Furthermore,
102 differential foliar damage (related to O_3 exposure) has been observed among sacred
103 fir (*Abies religiosa*) provenances in central Mexico (Hernández-Tejeda & Benavides-
104 Meza, 2015).

105 More than 5 million vehicles circulate daily in Mexico City (CDMX; INEGI,
106 2018), making it one of the most air-polluted cities in the world (ONU, 2018). Its
107 geographic location, mostly enclosed within a high-elevation valley, and the high
108 fossil fuel consumption generates perfect conditions for tropospheric O_3 formation
109 and accumulation (Bravo-Alvarez & Torres-Jardón, 2002; Molina et al., 2019). For
110 instance, while O_3 concentration in unpolluted air ranges between 20-50 ppb
111 (Seinfeld, 1989), daily levels in CDMX continuously reached 200 ppb during the
112 1990s (SEDEMA, 2020; Fig. 1a). Such elevated values still persist as isolated peaks
113 (reaching up to 180 ppb by 2017; SEDEMA, 2020; Fig. 1a), particularly between
114 March and June, when temperatures in CDMX are the highest and precipitation the
115 lowest (CONANP, 2006). Given that days with good air quality (*i.e.* <70 ppb) are still
116 scarce (Fig 1a) and that O_3 maxima are still well above the tolerable thresholds for
117 human and ecosystem health (NOM-020-SSA1-2104; SEDEMA Report, 2017), a
118 constant selective force with strong episodic peaks, that coincide with the start of the
119 growing season for most local plant species, is assumed to occur within the peri-
120 urban forests of CDMX.

121 Atmospheric drainage in CDMX mostly occurs between the southwestern
122 mountains, which are dominated by sacred fir forests (Fig. 1d; Alvarado-Rosales et
123 al., 2017). There is an ongoing decline of these forests, associated with the
124 detrimental effects of O_3 (de Bauer & Hernández-Tejeda, 2007), inadequate
125 management, excessive water extraction and recurrent forest fires (Alvarado R.,

1989; Macías-Sámano & Cibrían-Tovar, 1989). Firs within these forests exhibit O_3 damage in the form of reddish needles, which are rich in phenolic compounds and have degraded vacuoles and disintegrated spongy and palisade parenchyma (Alvarado-Rosales & Hernández-Tejeda, 2002; Alvarez et al., 1998). Damage becomes visible in one-year-old needles, which die after the third year of exposure. When compared to unpolluted areas of the species' range, such damage often leads to decreased vigour and increased susceptibility to several pests (Alvarado-Rosales & Hernández-Tejeda, 2002; Hernández-Tejeda & Benavides-Meza, 2015).

Although previous studies have described O_3 damage symptoms and pointed to this pollutant as the main cause for fir forest decline in CDMX (Alvarado R., 1989; Alvarado-Rosales & Hernández-Tejeda, 2002; de Bauer & Hernández-Tejeda, 2007), little attention has been paid to phenotypic differences for O_3-related symptoms until recently (Hernández-Tejeda & Benavides-Meza, 2015), when some apparently healthy young plants were observed within a heavily damaged stand. Complementing these observations in one of the most polluted cities of the world with methodological approaches to examine the effect of O_3 on plants can improve our understanding of how O_3 tolerance develops and operates in natural settings. For instance, at the histological level, we could expect more cellular damage in symptomatic trees than in asymptomatic individuals. Similarly, a deficient regulatory response to the oxidative stress caused by O_3 can be translated in the differential accumulation of certain metabolites, like some specific terpenes that have been observed in asymptomatic plants from various species after ozone exposure (Miyama et al., 2019; Kopaczyk et al., 2020). Lastly, transcriptomic analyses can help to narrow down the number of genes involved in the response to O_3 exposure

and to examine plastic responses in gene expression under varying levels of O_3 (DeBiasse & Kelly, 2016).

Here, we explored the differential histological, metabolomic (terpene) and transcriptomic responses to ozone pollution within a natural peri-urban forest dominated by *A. religiosa*. Given that previous reforestation attempts have been carried out in this zone, we first determined the geographic origin of individuals and then looked for differentially expressed genes between asymptomatic and symptomatic trees during days of high and relatively low ozone concentrations. This study represents a first step to guide peri-urban forest management from an eco-evolutionary perspective.

Material and methods

Study area and sampling

The study site is located near CDMX, in one of the most exposed areas to tropospheric ozone, the "Cruz de Coloxtitla" ravine, in the village of Santa Rosa Xochiac, next to the 'Desierto de los Leones' National Park (Alvarado-Rosales et al., 2017; Fig. 1d). We traced a quadrant of 80x137 m (19.285 N, -99.301 E; Fig. 2a) within this zone and focused on young (10-15 years old) *Abies religiosa* [(Kunth) Schlechtendahl et Chamisso] trees. We chose five plants exhibiting large numbers of reddish needles, indicative of damage by O_3 (Miller et al., 1994; hereafter referred to as "symptomatic" trees), as described elsewhere (Alvarado-Rosales & Hernández-Tejeda, 2002; Alvarez et al., 1998). Additionally, we selected five apparently healthy individuals, which had no visible damage in any branch ("asymptomatic" trees from hereon; Fig. 2-b, S2). Symptomatic and asymptomatic trees (n=10) were distributed heterogeneously within the zone and were separated by at least five meters from

each other (Fig. 2a). Needle samples were collected for each tree in three time points with contrasting O_3 concentration: moderate (April 15th, 2017; 87 ppb), intermediate (May 13-14th 2017, 120-94 ppb) and high (May 17th, 2017; 170 ppb; Fig. 1b-c), according to daily measurements from the nearest (PEDREGAL, PE) atmospheric station (available at http://www.aire.cdmx.gob.mx/default.php?opc=%27a8BhnmI=%27&opcion=Zg==). Needles were preserved in RNA Later and stored at -70°C until processing. The first sampling period roughly coincided with the start of the bud-burst period for this population (personal observations). Sampling was performed for all individuals between 13:30-15:30 hrs (Fig. 1c); needles were selected from three sections of the same branch, in six branches per individual. Each branch section corresponded to a particular growth period (*i.e.*, 2015, 2016 and 2017; Fig. 2b). No symptomatic individual had leaves more than three years old.

Genotyping and geographic origin of tolerant trees

Reforestation efforts in the study zone involved germplasm from foreign provenances (Hernández-Tejeda & Benavides-Meza, 2015). To verify that sampled plants originated locally, from natural regeneration, we employed previously published SNP data for 318 individuals from 19 populations of *A. religiosa* distributed across its natural range (Giles-Pérez et al., 2022). This data was used to assign the collected individuals to previously reported genetic clusters (Fig. 3a). To do so, we used 80 mg of needle tissue for DNA extraction using liquid nitrogen and the QUIAGEN DNeasy® Plant Mini Kit (cat. No. 69104), following the manufacturer's protocol. DNA integrity was checked in 1% agarose gel, and its concentration quantified with a Qubit™ v 3.0. Libraries were prepared following the protocol from

Poland & Rife (2012) after digestion with restriction enzymes *Msp*I (C | CGG) and *Pst*I (TGCA | G); a Pippin prep (SAGE sciences) was used to select the adequate fragment size before PCR amplification and sequencing. DNA sequencing was conducted in an Illumina's HiSeq2500 SE100 lane (100bp) and in a Nextseq lane (100 bp) were at the Institute of Integrative Biology and Systems at Université Laval, Canada (http://www.ibis.ulaval.ca/en/services-2/genomic-analysis-platform/). Read quality was examined using FastQC (http://www.bioinformatics.braham.ac.uk/projects/fastqc/) before and after demultiplexing and quality filtering. Reads were assembled *de novo*, and ipyrad was used for SNP calling (Eaton, 2014). Parameters used were: mindepth_statistical 8, mindepth_majrule 100000, clust_threshold 0.9. To optimize SNP calling, we followed the recommendations from Mastretta-Yanes et al. (2015), modified for ipyrad. We aimed keeping SNPs genotyped in at least 90% of individuals and with minor allele frequencies (MAF) above 0.05. Individuals with more than 10% missing data were discarded with PLINK1.9 (Purcell et al., 2007), and additional random individuals were removed until retaining only 3-5 trees of each population, along with the ten focus individuals of this study.

Pairwise relatedness between each pair of individuals within populations was calculated using PLINK 1.9 (Chang et al., 2015), as closely related individuals could bias further analyses, including population structure and assignment (Sethuraman, 2018). Only one of the focus (symptomatic) individuals was randomly discarded because of high relatedness (r>0.25) with another symptomatic tree (Fig. S3). ADMIXTURE v 1.3.0 (Bhatta et al., 2019) was used to infer population structure by supposing between 1 and 5 genetic clusters (*K*); optimal *K* was assumed to be the one with smallest cross validation error (CV).

Anatomical analyses

Transverse histological sections were prepared for five needles per branch from three branches of each tree, all sampled during the high O_3 concentration periods. Following sampling, needles were embedded in distilled water according to Sandoval et al. (2005) and cut in 7-10 mm sections. Sections were immersed overnight in a fixative solution composed of 50% ethanol, 10% formaldehyde, 35% double distilled water and 5% glacial acetic acid (FAA). After washing with distilled water and dehydration in a graded terbutylic alcohol series, sections were embedded in Paraplast ™, by adding 12-15 flakes every 30 min in an oven at 58 °C, until doubling the alcohol volume. Sections were stored at 56 ºC for 3 weeks until forming solid blocks (inclusion cubes), which were further sectioned with a rotating microtome (American Optical 820; 12µm). Ten to 15 transversal tissue sections were obtained per needle. The sections were first hydrated and dyed with safranin, then dehydrated within a graded ethanol series and stained with dye fast green (FCF), using a previously standardized method for sacred fir (Sandoval et al., 2005). Afterwards, they were mounted on slides and dried for 15 days in an oven at 56° C. We looked for cell structures previously reported as symptoms of O_3 damage (Fig. S2; Gimeno & Ibars, 2009). Samples were photographed in an Axioskope Car Zeiss photomicroscope for examining tissue-level damage, compared to a reference description of *A. religiosa* (Alvarez et al., 1998)**.**

Terpenes analysis

Two- and three year-old needles (corresponding to the growth years of 2015 and 2016) collected during moderate (87 ppb) and high (170 ppb) O_3 concentration

periods were used to quantify relative terpene abundances (Ibrahim et al., 2019). Approximately 80-95 mg (fresh-weight) tissue preserved in liquid nitrogen was macerated with a mortar and pestle with 2 mL of dichloromethane, transferred to microtubes, and centrifuged (within tubes) for 1 min at 14,000 rpm. The supernatant was recovered and dried with compressed air, and the pellet was resuspended in 450 µl of dichloromethane and 50 µl of 1mg/mL 1-isopropylphenol (as internal standard). After homogenization, 2 µl were injected into a gas chromatograph with a Split/splitless injector (Agilent Technologies 6850 Network GC System) coupled to a mass spectrometer (5975C VL MSD with Triple-Axis Detector) and a Xylan (Quadrex) 30 m * 0.25 mm * 0.25 µm capillary column. Analyses were performed at 230°C in the splitless mode (3 min). The initial temperature was set at 70°C for 2 min, then increased to 230°C at a rate of 20° C / min, and maintained for 5 min. Helium (*i.e.,* carrier gas) was injected at a rate of 1 mL / min; the temperatures of the transfer line, ionization source, and quadrupole analyzer were 280°C, 230°C, and 150°C, respectively. Analyses were performed by electronic impact at 70 eV using the full spectrum scan mode (SCAN). For relative quantification, peak areas were integrated and normalized to the internal standard. Each peak (associated to a specific metabolite) was validated according to its retention time and mass spectrum based on the National Institute of Standards and Technology (NIST) library.

Only terpenes with similar fragmentation patterns or retention times (TR), observed in at least 60 % of the samples and with at least 80% identification probability were retained. A matrix of relative abundance per 100 g of tissue was then generated for comparison between tree conditions (asymptomatic vs. symptomatic), periods (high and moderate O_3), and needle age (2015, 2016; Fig. 1) through a linear model using R (R Core Team, 2021), assuming a Gamma

distribution. We compared the goodness of fit of the models with the Akaike's information criterion. The better model was Metabolites Concentration ~ Condition * Period. We performed non-paired comparisons, with Wilcoxon tests, to explore variations in metabolite composition between asymptomatic and symptomatic groups, between periods (87 ppb vs 170 ppb) and needle ages (one year vs two years). Analyses were performed in the stats package 4.1.2 (R Core Team, 2021) and results were visualized with ggplot2 3.3.5 (Wickham, 2016).

Differential expression analyses

One- and two-year old needles (2015 and 2016) sampled during the moderate (87 ppb) and high (170 ppb) O_3 concentration periods were further analyzed for differential expression through RNA sequencing. Total RNA was isolated using a Spectrum RNA Plant™ kit (cat. No. STRN50, SIGMA) from 40 to 45 mg of tissue. RNA integrity was evaluated by 1% agarose gel electrophoresis, and its quality and purity were determined using NanoDrop (ultradifferential spectrophotometer) according to the 260/280 and 260/230 ratios. RNA concentration was quantified with a Qubit ™ RNA IQ assay (Invitrogen). The 18 sequencing libraries from poly(A)+ enriched RNA (Table S5) were prepared, and then sequenced in a Hi-Seq 4000 in a 150PE sequencing lane at the University of Berkeley, USA (https://www.berkeley.edu/).

Demultiplexing was performed by the sequencing service. We performed quality checks with FastQC and removed adapters and low-quality reads with

297 Trimmomatic (Bolger et al., 2014) using the following parameters: -phred33,
298 ILLUMINA CLIP: TruSeq3-PE-2.fa: 2: 30: 10, LEADING: 3, TRAILING: 3, SLIDING
299 WINDOW: 10 MINLEN: 50. Reads were mapped to the *Abies balsamea*
300 transcriptome (Van Ghelder et al., 2019; Bioproject PRJNA437248 in Genbank) with
301 BWA-MEM (Li & Durbin, 2009). Once the reads were mapped, we quantified the
302 transcript abundance by counting the mapped reads per transcript for each sample
303 (Table S6). Differential expression analyses were performed with DESeq2 (Love
304 et al., 2014) and edgeR (Robinson et al., 2010) in R for the following comparisons:
305 (1) symptomatic vs. asymptomatic individuals during the high O_3 concentration
306 period (170 ppb); (2) asymptomatic trees during the moderate (87ppb) vs. high O_3
307 concentration (170ppb) periods; and (3) symptomatic individuals during the
308 moderate (87ppb) vs. high O_3 concentration (170ppb) periods.
309 Transcripts with *p*-values lower than 0.005, after fold change correction
310 (Benjamini et al., 2001), were considered differentially expressed. Only those
311 transcripts detected by both methods were retained and analysed for identifying the
312 most likely open reading frames. They were then annotated with TRAPID 2.0 (Van
313 Bel et al., 2019) and BLASTx (https://blast.ncbi.nlm.nih.gov/Blast.cgi) using the
314 non-redundant database (nr); we retained the first five hits for each transcript. For
315 those transcripts that could not be annotated, we performed BLASTx searches
316 against theGymnosperm transcriptomes available at the Congenie
317 database(congenie.org). Proteins of annotated transcripts were finally assigned to
318 their respective metabolic pathways using KOALA (KEGG Orthology And Links
319 Annotation (Kanehisa et al., 2016).
320
321 **Results**

Genotyping and geographic origin of trees

After *de novo* assembly and filtering, 1,550 SNPs were genotyped for the 88 retained *A. religiosa* individuals distributed along most of its range (Giles-Pérez et al., 2022), and for the ten focus samples of this study. Although the optimal number of genetic clusters (*K*) for the Admixture analysis was 2, a higher value (K = 5) had a better resolution for differentiating groups in the eastern and western most parts of the species distribution, allowing individual assignment. Both the symptomatic and asymptomatic trees of this study were assigned to the central-Mexico cluster, to which trees from neighboring populations, such as Ajusco and Nevado de Toluca also belong (Fig. 3). This result indicates that only local germplasm was included in our study.

Anatomical differentiation

Tissue differences were found between symptomatic and asymptomatic trees and among growth years (*i.e.,* needles developed in 2015 and 2016 and sampled in 2017) within individuals (Fig. 2b, Fig. S2). Needles of symptomatic trees exhibited a thicker epidermis and more collapsed cells than those of the asymptomatic ones, mainly within the palisade parenchyma (Fig. 2b). In contrast, the spongy parenchyma, resin channels and vascular tissues looked similar in the needles of symptomatic and asymptomatic individuals. Cell collapse became more evident with needle age in symptomatic trees (*i.e.,* higher for 2015 than for 2016 needles), while asymptomatic individuals showed less cell collapse in the two-year-old needles (2015) than in the one-year-old needles (2016; Fig. 2b).

Terpenes analysis

Compounds identified in all extracts included: ∂-cadinene, α-cubebene, ß-cubebene, α-caryophyllene, ß-caryophyllene oxide, L-α-bornyl acetate, and ß-pinene (Fig. 4). The best model for explaining the differences in concentration of these shared terpenes (Nagelkerke's R2 = 0.645), indicated an association with the tree's condition (symptomatic and asymptomatic) and the period of exposition (87 ppb vs 170 ppb), with needle age being less relevant. Indeed, concentrations of all shared terpenes exhibited significant differences ($p < 0.001$, $p < 0.01$, or 0.05, Fig. 4) between symptomatic and asymptomatic individuals during the period of moderate ozone concentration. In addition, there were statistical differences in the terpene concentrations of asymptomatic trees between periods (87 ppb vs 170 ppb), but no differences were found between periods for the symptomatic trees or between needle ages (one- or two-years).

Differential expression analyses (RNA-seq)

After quality filtering, 605,147,387 paired reads were retained for 18 samples, with an average of 33,619,299 reads per sample. The percentage of reads mapped to the reference transcriptome (*A. balsamea*) ranged between 84.5 % and 96.7% per sample (Table S6), indicating excellent transcript coverage. Eleven differentially expressed transcripts were identified in the needles of the symptomatic and asymptomatic trees (fold change) during the high O_3 concentration period using both the DESeq2 and edgeR methods (Fig. 5a). Five of them were upregulated and six were downregulated in asymptomatic individuals. Six of these transcripts could be

annotated (Table S1) and were involved in carbohydrate metabolism, gene regulation, and defense, according to KOALA. All of these transcripts belong to gene families whose members are involved in different aspects of abiotic and biotic stress response (see Table S1 for details), four of which have been previously associated with O_3 response in controlled experiments with plants: *LRR receptor-like protein kinases* (two annotated transcripts), an *L-type lectin-domain containing receptor kinase*, and a *chitinase* (Table S1).

When comparing transcript expression between trees with the same phenotype collected during low and high O_3 concentration periods, we observed six and twenty-two differentially expressed transcripts for the symptomatic and asymptomatic individuals, respectively; 17 of which could be annotated (Fig. 5b-c, Table S2-3). Remarkably, the number of differentially expressed transcripts in the asymptomatic plants was almost four times higher than that in symptomatic trees.

Among the five upregulated transcripts differentially expressed between periods in the symptomatic individuals, two transcripts were involved in the regulation of gene expression (encoding a *NAC* transcription factor and histone 1.3 variant) and one was involved in cell wall remodeling (encoding a *xyloglucan endotransglucosylase*). The only downregulated transcript for these symptomatic trees encoded an enzyme from the *UDP-glucosyl transferase* family involved in various metabolic processes, including flavanol, tetrapyrrole, and terpene biosynthesis (Table S2). Homologues in other plant species for four of the upregulated transcripts have been previously associated with ozone response, including the abovementioned *NAC* transcription factor and UDP- *glucosyl transferase* (Table S2).

For the asymptomatic trees, 16 of the 22 differentially expressed transcripts between periods could be annotated (Table S3). For two of them, no homologous amino acid sequences were found, but the results of BLASTn performed in the Congenie database suggest that these could respectively represent a conifer specific non-coding RNA, and a conifer-specific peptide or protein. As for the annotated transcripts of these symptomatic individuals, they belong to gene families involved in response to abiotic and biotic stress, and the regulation of gene expression, four of these transcripts have been reported in controlled O_3 experiments in plants (Table S3). Interestingly, these include the *linker histone H1*, which was also upregulated in the symptomatic trees during the high O_3 concentration period.

Discussion

In this study, we explored the histological, metabolomic, and transcriptomic changes between symptomatic and asymptomatic fir trees within a natural population that has been heavily exposed to tropospheric O_3 for over 40 years. According to our genetic ancestry analysis, all the studied individuals belong to the local gene pool, which suggests that the observed differences are the likely result of intrinsic evolutionary processes within this population. Such differences include histological traits whose disparity increases with needle age, and contrasting terpene composition and gene expression. Our results illustrate how signals of O_3 tolerance can arise in a natural population after a few decades of frequent exposure and shed light on the metabolic and gene regulation mechanisms involved in conifers.

Asymptomatic trees have a local genetic origin

Comparing the genetic ancestry of our focus trees with other populations allowed us to confidently assign them to the previously reported central-Mexican genetic cluster (Giles-Pérez et al., 2022; Fig. 3b). This is important given that various reforestation efforts with foreign germplasm have been performed in the study zone and that some provenances have shown differential sensitivity to O_3 (Hernández-Tejeda & Benavides-Meza, 2015). Given that reforested trees have still not reached reproductive maturity, O_3 tolerance at the study site is the likely product of local processes, based on either plasticity or standing genetic variation (see below). Should genetic factors be involved, we hypothesize that only a relatively large effective population size could allow for the rapid evolutionary changes that are necessary to respond to such a strong environmental pressure in such a short term (1-2 generations if we consider a generation time of 25 years for sacred fir). Detailed quantitative and population genomics studies are thus necessary to evaluate tolerance heritability, estimate demographic parameters, and pinpoint the genomic bases of such putative adaptation.

Histological O_3 damage begins after only a few days of exposure

Overall, the symptoms observed herein were similar to those reported for other plant species experimentally exposed to O_3 under controlled conditions, at both the macroscopic and histological levels (Chaudhary & Rathore, 2021; Moura et al., 2022). Such symptoms are different from those expected from other possible stresses, such as drought or disease, which produce yellowish needles and a more homogeneously affected foliage (including needle loss; Chastagner, 2001; Johnson et al., 2005). In contrast, in this study, the reddish needle symptoms indicative of O_3

440 damage were first observed in 2-year-old needles, and foliage loss was limited to 3-
441 year-old or older needles.
442 At the histological level, the needles of all individuals bore signs of damage,
443 albeit to a much lower degree for the asymptomatic trees than for the symptomatic
444 individuals (Fig. 2b, S2). This suggests a multivariate response to O_3 exposure that
445 results in a continuous rather than in a discrete phenotype, likely controlled by
446 polygenic or epigenetic factors. Our data further shows that O_3 damage begins at the
447 tissue level during the first 30 days after bud burst (2017 buds; Fig. 2b), even if
448 symptoms are still not noticeably macroscopically. Such precocious signs have been
449 described for other conifers, for which they could appear as early as the fifth day of
450 exposure (Evans & Fitzgerald, 1993). Both the visible and histological damages in
451 firs aggravate with needle age (Fig. 2), which indicates a cumulative and irreversible
452 effect of O_3 exposure (Schraudner et al., 1998), similar to that reported in controlled
453 experiments in other plant species (Lee et al., 2020).
454 Cell collapse was particularly important within the palisade parenchyma (Fig.
455 2b, S2; (Alvarez et al., 1998; Evans & Fitzgerald, 1993; Terrazas & Bernal-Salazar,
456 2002), which has been attributed to oxidizing agents that act on the middle lamella of
457 the cell wall and promote its degradation (Gimeno & Ibars, 2009). Such degradation
458 increases intercellular spaces and leads to cell death (Alvarez et al., 1998), and it is
459 often accompanied by the accumulation of phenolic and tannin compounds that
460 produce the characteristic reddish coloration of O_3 damage (Fig. 2b, S2; (Gostin,
461 2010).
462 Symptomatic individuals had thicker epidermis than asymptomatic individuals
463 (Ep; Fig. 2b). Such thickening has already been associated with O_3 response in
464 conifers (Kivimäenpää et al., 2017) and might indicate increased synthesis of cell

wall components under O_3 stress (Sandermann et al., 1997). Interestingly, we did not find any differences in cuticle and resin duct structure between symptomatic and asymptomatic trees (Fig. 2b, S2), which was reported as a recurrent sign of O_3 damage in pines (Vollenweider et al., 2003). This suggests that either firs have a greater tolerance to O_3 than pines or that such symptoms can only be observed when comparing individuals unexposed and exposed to O_3 (which was impossible to settle in our study, because there are no zero-exposure periods in our study site throughout the year). Our own casual field observations suggest that pines (*i.e., Pinus ayacahuite, P. harwegii* and *P. veitchii*) growing in the study site seem to be more affected than firs in terms of mortality, needle loss, and needle coloration.

Asymptomatic trees produce terpenes related to response to biotic and abiotic stress and recovery after stress

Changes in cell structure in ozone-damaged plants may result from rampant oxidative stress (Baier et al., 2005; Iriti & Faoro, 2008). These may be produced by a deficient regulatory response, which results in the differential accumulation of certain metabolites, including terpenes (Kopaczyk et al., 2020; Miyama et al., 2019). Although we observed no clear anatomical differences in the resin ducts between symptomatic and asymptomatic trees, which could have indicated contrasting metabolite accumulation (Fig. 4), there were significant differences in terpene composition, particularly sesquiterpenes, between asymptomatic and symptomatic phenotypes during the moderate O_3 period. This is particularly compelling because sesquiterpenes, which were also found to increase their concentration in angiosperms when exposed to O_3 (Kanagendran et al., 2018; Pellegrini et al., 2012),

have been shown to degrade reactive oxygen species (ROS) and reduce cellular damage (Loreto & Fares, 2007; Vickers et al., 2009).

In our study, sesquiterpenes such as ß-pinene, Δ-cadinene and ß-caryophyllene were observed at higher concentrations in the asymptomatic than the asymptomatic trees prior to the high O_3 concentration period (Fig. 4). Such compounds have been associated with antioxidant and larvicidal functions in several plant species, including pines (Govindarajan et al., 2016; Kanagendran et al., 2018; Loreto et al., 2004; Ortiz de Elguea-Culebras et al., 2017). These terpenes could be allowing the asymptomatic trees to better cope with biotic and abiotic stresses once O_3 exposure increases (Pellegrini et al., 2012). The whole biosynthetic pathway leading to these compounds should be of particular interest for future functional and evolutionary studies in firs and other plants. However, given that insects often attack already weakened trees (like those exposed to O_3), such studies should also focus on disentangling the metabolic response to ozone exposure and insect defense.

Asymptomatic trees further produced a larger quantity of metabolites related to recovery after stress than symptomatic plants when we compared the metabolite composition between moderate and high O_3 periods (Fig. 4). Particularly β-pinene, which has been previously related to the plant recovery after a high O_3 exposure in *Nicotiana tabacum* (Kanagendran et al., 2018). This reinforces the idea that O_3 exposure is the main cause of forest degradation at our study site.

The members of the family of *UDP-glycosyltransferase* (UGT) enzymes participate in terpene biosynthesis (AB_008838_T.1; Table S2) . The lower concentration of terpenes during the high O_3 period (Fig. 4) may be associated with the down-regulalation of these transcripts in symptomatic trees when comparing the low (87 ppb) and high (170 ppm) O_3 concentration periods (Table S2). However, our

study should be complemented by examining the concentration of other metabolites, like flavonoids or tannins, in the future. Indeed, our results indicated that the expression of transcripts involved in the flavonoid metabolic pathway could exhibit considerable differences compared with those found for terpene metabolism, as demonstrated by the transcriptomic data (AB_000811_T.1; Table S1). In any case, the metabolic signatures reported here could already be used to identify trees that are not adequately recovering after O_3 exposure in affected forests.

Transcripts related to stomatal opening and response to stress are up-regulated in asymptomatic trees

To further examine the molecular basis of O_3 response, we performed a differential transcript expression analysis (DTE). We found differentially expressed transcripts when comparing asymptomatic and symptomatic trees during the high O_3 concentration period (Table S1, Fig. 5a) and when independently comparing concentration periods for individuals with the same phenotype (Table S2-S3, Fig. 5b-c). Homologs of several of these transcripts have been previously reported as differentially expressed in controlled O_3 exposure experiments in angiosperms (Natali et al., 2018; Tammam et al., 2019; Waldeck et al., 2017), which suggests that the molecular mechanisms underlying response to O_3 are conserved on a large evolutionary time scale.

The differentially expressed transcripts during high O_3 concentration periods were associated with defense against pathogens and stomata opening, and included transcripts related to chitinases and LRR protein kinases. These proteins are known to play important roles in recognizing and responding to pathogens in plants (Vaghela et al., 2022; Wang et al., 2023), and their differential expression suggests

539 either a response to an unaccounted pathogen attack (e.g., fungi) or that this
540 signaling pathway is activated under both O_3 exposure and other stressors. Again,
541 this indicates the need for further studies to disentangling the response to O_3 and
542 biotic stress defense. Interestingly, some members of the LRR kinases gene family
543 are also associated with the initial physiological reaction of plants to O_3 exposure,
544 which involves stomatal closure (Hasan et al., 2021). Thus, studying stomata
545 closure, and its underlying genes, should be a priority for future studies in natural
546 plant populations affected by O_3 pollution.

547 Comparing transcriptional profiles among trees with the same phenotype,
548 asymptomatic or symptomatic, also showed differential responses to increased O_3
549 concentration. In other words, the upregulated and downregulated transcripts belong
550 to different GO categories. Among the upregulated transcripts in symptomatic
551 individuals during the moderate O_3 period (Fig. 5b, Table S2), a homolog of the
552 *xyloglucan endo*-transglycosylase and a *non-apical meristem* (NAM) transcription
553 factor from the large NAC family stand out, as some of their homologs have been
554 shown to play a key role in cell repair after O_3 exposure (Zhang et al., 2017) and are
555 activated by O_3 during apoplastic ROS signaling (De Clercq et al., 2013). The
556 activation of these pathways in symptomatic trees when O_3 concentration is low,
557 might be indicative of decreased sensitivity to this pollutant when compared to the
558 asymptomatic trees.

559 During the high O_3 period, asymptomatic individuals upregulated some
560 transcripts (Fig. 5c, Table S3) related to plant resistance (NB-ARC-domain proteins),
561 plant defense (peroxidases), and the flavonoid biosynthesis (chalcones) pathway
562 (Dao et al., 2011; Krasensky et al., 2017). In other words, when O_3 concentration
563 increases, asymptomatic trees may be activating mechanisms related to stress

response. Moreover, transcripts encoding for *UDP-glycosyltransferase (UGT)* family members (Fig. 5b, Table S2), which are essential components of the plant secondary metabolism pathway that helps detoxify harmful compounds (Pan et al., 2019), are downregulated in asymptomatic trees. *UGTs* are also essential for regulating various aspects of plant growth and development (Mateo-Bonmatí et al., 2021).

All in all, the variety of pathways differentially activated between symptomatic and asymptomatic trees highlights the complexity of studying plant transcriptomic responses in natural conditions (Nunn et al., 2006). Indeed, several sources of stress are expected to act at the same time in degraded forests subjected to air pollution. To disentangle the various mechanisms involved, it is advisable to use controlled experiments, such as ozone top chambers (Abeyratne & Ileperuma, 2006; Palomäki et al., 1998), in combination with *in situ* studies in natural settings to understand how plants respond to stress under real-life scenarios. However, although several sources of stress are at play in peri-urban forests of Mexico City, our histological, terpenes, and transcriptomic analyses confirm that O_3 pollution is an important stressor that triggers a rapid and differential phenotypic response in firs, likely modeled by standing genetic variation and/or plastic mechanisms. The evolutionary basis of such differences remains open to be explored. Since epigenetic variation is related to gene activity and expression (Richards et al., 2017; Srikant & Drost, 2021), and can accumulate faster than DNA mutations, their role in the phenotypic response to O_3 pollution must be addressed in future studies.

Data accessibility and benefit-sharing

Histological images and processed terpenes, genotype (vcf files) and transcriptomic (expression tables) data are available at the Dryad repository XXXXX (available upon acceptance). Pipelines and code for all analyses is available at the Github repository (https://github.com/VeroIarrachtai/Abies_religiosa_vs_ozone). Transcriptome raw sequences data were deposited in GeneBank under accession numbers XXXX (available upon acceptance). Demultiplexed sequencing data, including those samples previously analyzed in a phylogenetic survey (i.e., 80 samples, Giles et al.,2022), were deposited in NCBI with the Bioproject ID: PRJNA856692; while filtered variant files used for population genomic analyses, code and pipelines are hosted on Dryad Repository at XXXX (available upon acceptance) and on GitHub at XXXX (available upon acceptance).

Author contributions

VRG, CZC and AMY performed sampling. VRG performed lab work and analyses. VRG, JPJC and AMY designed the study, interpreted results, and drafted the manuscript. LS, CAM, SS, ESZ, RTJ, CMF and DP contributed to data analyses and interpretation. All authors produced and approved the final version of the manuscript.

Acknowledgements

We thank Héctor Mario Benavides-Meza, INIFAP, and the community of Bienes Comunales Santa Rosa Xochiac, Mexico, for field assistance. We are grateful to T. Garrido-Garduño, A. Guerra and N. Galvez-Reyes for laboratory assistance. Analyses were carried out on CONABIO's computing cluster, supported by Ernesto Campos Murillo and the ‘Subcoordinación de Soporte Informático’.

This project was financially supported by grants from the “Consejo Nacional de Ciencia y Tecnología” (CONACyT; National Problems-247730 to AM-Y; CB-2016-284457 and COOB2016-01-278987 to JPJ-C), the “Dirección General de Asuntos del Personal Académico at UNAM (PAPIIT IN224723) and the internal budget of IE-UNAM, both to JPJ-C. This work is part of the MSc thesis of VR-G at the ‘Programa de Maestría en Ciencias Biológicas, Universidad Nacional Autónoma de México’ who further thanks the support of Consejo Nacional de Ciencia y Tecnología through a MSc Scholarship (no. 714560).

References

Abeyratne, V. D., & Ileperuma, O. (2006). *OPEN-TOP CHAMBER METHOD TO ASSESS THE POTENTIAL VISIBLE SYMPTOMS ON FOLIAGE OF ANNUAL CROP PLANTS EXPOSED TO OZONE*. https://www.semanticscholar.org/paper/OPEN-TOP-CHAMBER-METHOD-TO-ASSESS-THE-POTENTIAL-ON-Abeyratne-Ileperuma/44bfd89191b2009351802b8bd3b1460fb8283722

Alvarado R., D. (1989). *Declinación y muerte del bosque de oyamel (Abies religiosa) en el sur del Valle de México*. Colegio de Posgraduados, Campus Montecillo (México). Institución de Enseñanaza e Investigación en Ciencias Agrícolas. Centro de Fitopatología.

Alvarado-Rosales, D., de Lourdes Saavedra-Romero, L., Hernández-Tejeda, T., Cox, R. W., & Malcolm, John. W. (2017). *Concentraciones in situ de ozono en bosques de la Cuenca de México e influencia de la altitud*. *8*(44), 29-54.

636 Alvarado-Rosales, D., & Hernández-Tejeda, T. (2002). *Decline of Sacred Fir in the*
637 *Desierto de los Leones National Park*. 243-260.

638 Alvarez, D., Laguna, G., & Rosas, I. (1998). Macroscopic and microscopic symptoms
639 in Abies religiosa exposed to ozone in a forest near Mexico City.
640 *Environmental Pollution*, *103*(2), 251-259.

641 Ashmore, M. (2005). Assessing the future global impacts of ozone on vegetation.
642 *Plant Cell and Environment*, *28*(8), 949-964.

643 Bai, X., McPhearson, T., Cleugh, H., Nagendra, H., Tong, X., Zhu, T., & Zhu, Y.-G.
644 (2017). Linking Urbanization and the Environment: Conceptual and Empirical
645 Advances. *Annual Review of Environment and Resources*, *42*(1), 215-240.

646 Baier, M., Kandlbinder, A., Golldack, D., & Dietz, K.-J. (2005). Oxidative stress and
647 ozone: Perception, signalling and response. *Plant, Cell & Environment*, *28*(8),
648 1012-1020.

649 Benjamini, Y., Drai, D., Elmer, G., Kafkafi, N., & Golani, I. (2001). *Controlling the*
650 *false discovery rate in behavior genetics research*. *125*(1-2), 279-284.

651 Berrang, P., Karnosky, D. F., Bennett, J. P., & J. P. Bennett. (1991). Natural
652 selection for ozone tolerance in Populus tremuloides: An evaluation of
653 nationwide trends. *Canadian Journal of Forest Research*, *21*(7).

654 Bhatta, M., Morgounov, A., Belamkar, V., Wegulo, S. N., Dababat, A. A., Erginbas-
655 Orakci, G., Bouhssini, M. E., Gautam, P., Poland, J., Akci, N., Demir, L.,
656 Wanyera, R., & Baenziger, P. S. (2019). Genome-Wide Association Study for

Multiple Biotic Stress Resistance in Synthetic Hexaploid Wheat. *International Journal of Molecular Sciences*, *20*(15), 3667.

Bhaumik Vaghela, Rahul Vashi, Kiransinh Rajput, & Rushikesh Joshi. (2022). Plant chitinases and their role in plant defense – a comprehensive review. *Enzyme and microbial technology*, 110055-110055.

Bravo-Alvarez, H., & Torres-Jardón, R. (2002). Air Pollution Levels and Trends in the Mexico City Metropolitan Area. En M. E. Fenn, L. I. de Bauer, & T. Hernández-Tejeda (Eds.), *Urban Air Pollution and Forests: Resources at Risk in the Mexico City Air Basin* (pp. 121-159). Springer.

Chang, Y.-C., Lo, H.-H., Hsieh, H.-Y., & Chang, S.-M. (2015). Identification, epidemiological relatedness, and biofilm formation of clinical Chryseobacterium indologenes isolates from central Taiwan. *Journal of Microbiology, Immunology, and Infection = Wei Mian Yu Gan Ran Za Zhi*, *48*(5), 559-564.

Chastagner, G. A. (2001). Susceptibility of Intermountain Douglas-Fir to Rhabdocline Needle Cast When Grown in the Pacific Northwest. *Plant Health Progress*, *2*(1), 2.

Chaudhary, I. J., & Rathore, D. (2021). Micro-morphological and anatomical response of groundnut (Arachis hypogaea L.) cultivars to ground-level ozone. *Journal of Applied Biology and Biotechnology*, *9*(4), 137-150.

Cho, K., Tiwari, S., Agrawal, S. B., Torres, N. L., Agrawal, M., Sarkar, A., Shibato, J., Agrawal, G. K., Kubo, A., & Rakwal, R. (2011). Tropospheric Ozone and Plants: Absorption, Responses, and Consequences. En D. M. Whitacre (Ed.),

Reviews of Environmental Contamination and Toxicology Volume 212 (Vol. 212, pp. 61-111). Springer New York.

Churkina, G., Kuik, F., Bonn, B., Lauer, A., Grote, R., Tomiak, K., & Butler, T. M. (2017). Effect of VOC Emissions from Vegetation on Air Quality in Berlin during a Heatwave. *Environmental Science & Technology*, *51*(11), 6120-6130.

CONANP. (2006). *Programa de Conservacion y Manejo Parque Nacional Desierto de los Leones.*

Dao, T. T. H., Linthorst, H. J. M., & Verpoorte, R. (2011). Chalcone synthase and its functions in plant resistance. *Phytochemistry Reviews*, *10*(3), 397-412.

de Bauer, M. de L., & Hernández-Tejeda, T. (2007). A review of ozone-induced effects on the forests of central Mexico. *Environmental Pollution*, *147*(3), 446-453.

De Clercq, I., Vermeirssen, V., Van Aken, O., Vandepoele, K., Murcha, M. W., Law, S. R., Inzé, A., Ng, S., Ivanova, A., Rombaut, D., van de Cotte, B., Jaspers, P., Van de Peer, Y., Kangasjärvi, J., Whelan, J., & Van Breusegem, F. (2013). The Membrane-Bound NAC Transcription Factor ANAC013 Functions in Mitochondrial Retrograde Regulation of the Oxidative Stress Response in Arabidopsis. *The Plant Cell*, *25*(9), 3472-3490.

DeBiasse, M. B., & Kelly, M. W. (2016). Plastic and Evolved Responses to Global Change: What Can We Learn from Comparative Transcriptomics? *Journal of Heredity*, *107*(1), 71-81.

Eaton, D. A. R. (2014). PyRAD: Assembly of de novo RADseq loci for phylogenetic analyses. *Bioinformatics*, *30*(13), 1844-1849.

Evans, L. S., & Fitzgerald, G. A. (1993). Histological effects of ozone on slash pine (Pinus elliotti var. Densa). *Environmental and Experimental Botany*, *33*(4), 505-513.

Felzer, B. S., Cronin, T., Reilly, J. M., Melillo, J. M., & Wang, X. (2007). Impacts of ozone on trees and crops. *Comptes Rendus Geoscience*, *339*(11-12), 784-798.

Giles-Pérez, G. I., Aguirre-Planter, E., Eguiarte, L. E., & Jaramillo-Correa, J. P. (2022). Demographic modelling helps track the rapid and recent divergence of a conifer species pair from Central Mexico. *Molecular Ecology*, *31*(19), 5074-5088.

Gimeno, D. L., & Ibars, A. M. (2009). Impacto del ozono troposférico sobre la anatomía foliar de Abies pinsapo Boiss. I: Estudio de la distribución de daños. *Acta Botanica Malacitana*, *34*, 175-188.

Gostin, I. (2010). Structural changes in silver fir needles in response to air pollution. *Analele Unive rsităţii din Oradea*, *17*(2), 300-305.

Govindarajan, M., Rajeswary, M., & Benelli, G. (2016). Chemical composition, toxicity and non-target effects of Pinus kesiya essential oil: An eco-friendly and novel larvicide against malaria, dengue and lymphatic filariasis mosquito vectors. *Ecotoxicology and Environmental Safety*, *129*, 85-90.

722 Hasan, M., Hasan, M., Rahman, A., Rahman, A., Md. Atikur Rahman, Skalicky, M.,
723 Alabdallah, N. M., Waseem, M., Waseem, M., Jahan, M. S., Ahammed, G. J.,
724 El-Mogy, M. M., El-Yazied, A. A., Ibrahim, M. F. M., Xiang-Wen Fang, & Fang,
725 X.-W. (2021). Ozone Induced Stomatal Regulations, MAPK and
726 Phytohormone Signaling in Plants. *International Journal of Molecular*
727 *Sciences*, *22*(12), 6304.

728 Hayes, F., Harmens, H., Sharps, K., & Radbourne, A. (2020). Ozone dose-response
729 relationships for tropical crops reveal potential threat to legume and wheat
730 production, but not to millets. *Scientific African*, *9*, e00482.

731 Hernández-Tejeda, T., & Benavides-Meza, H. M. (2015). *Sensitivity of 20*
732 *provenances of pine and Sacred fir to photochemical oxidants. 6*(30), 32-51.

733 INEGI, (2018). https://www.inegi.org.mx

734 Iriti, M., & Faoro, F. (2008). Oxidative Stress, the Paradigm of Ozone Toxicity in
735 Plants and Animals. *Water, Air, and Soil Pollution*, *187*(1), 285-301.

736 Jáuregui, E. (2002). *The Climate of the Mexico City Air Basin: Its Effects on the*
737 *Formation and Transport of Pollutants* (pp. 86-117).

738 Johnson, G. R., Grotta, A. T., Gartner, B. L., & Downes, G. (2005). Impact of the
739 foliar pathogen Swiss needle cast on wood quality of Douglas-fir. *Canadian*
740 *Journal of Forest Research*, *35*(2), 331-339.

741 Johnson, M. T. J., & Munshi-South, J. (2017). Evolution of life in urban
742 environments. *Science*, *358*(6363).

743 Kanagendran, A., Pazouki, L., Li, S., Liu, B., Kännaste, A., & Niinemets, Ü. (2018).
744 Ozone-triggered surface uptake and stress volatile emissions in Nicotiana
745 tabacum ‘Wisconsin’. *Journal of Experimental Botany*, *69*(3), 681-697.

746 Kanehisa, M., Sato, Y., Kawashima, M., Furumichi, M., & Tanabe, M. (2016). KEGG
747 as a reference resource for gene and protein annotation. *Nucleic Acids*
748 *Research*, *44*(D1), D457-462.

749 Kivimäenpää, M., Sutinen, S., Valolahti, H., Häikiö, E., Riikonen, J., Kasurinen, A.,
750 Ghimire, R., Holopainen, J., & Holopainen, T. (2017). Warming and elevated
751 ozone differently modify needle anatomy of Norway spruce (Picea abies)
752 and Scots pine (Pinus sylvestris). *Canadian Journal of Forest Research*, *47*,
753 488-499.

754 Kopaczyk, J. M., Warguła, J., & Jelonek, T. (2020). The variability of terpenes in
755 conifers under developmental and environmental stimuli. *Environmental and*
756 *Experimental Botany*, *180*, 104197.

757 Krasensky, J., Carmody, M., Sierla, M., & Kangasjärvi, J. (2017). *Ozone and*
758 *Reactive Oxygen Species*. 1-9.

759 Lee, J. K., Woo, S. Y., Kwak, M. J., Park, S. H., Kim, H. D., Lim, Y. J., Park, J. H., &
760 Lee, K. A. (2020). Effects of Elevated Temperature and Ozone in Brassica
761 juncea L.: Growth, Physiology, and ROS Accumulation. *Forests*, *11*(1), Article
762 1.

763 Li, H., & Durbin, R. (2009). Fast and accurate short read alignment with Burrows-
764 Wheeler transform. *Bioinformatics (Oxford, England)*, *25*(14), 1754-1760.

765 Loreto, F., & Fares, S. (2007). Is Ozone Flux Inside Leaves Only a Damage
766 Indicator? Clues from Volatile Isoprenoid Studies. *Plant Physiology*, *143*(3),
767 1096-1100.

768 Loreto, F., Pinelli, P., Manes, F., & Kollist, H. (2004). Impact of ozone on
769 monoterpene emissions and evidence for an isoprene-like antioxidant action
770 of monoterpenes emitted by Quercus ilex leaves. *Tree Physiology*, *24*(4), 361-
771 367.

772 Love, M. I., Huber, W., & Anders, S. (2014). Moderated estimation of fold change
773 and dispersion for RNA-seq data with DESeq2. *Genome Biology*, *15*(12), 550.

774 Ludwików, A., & Sadowski, J. (2008). Gene Networks in Plant Ozone Stress
775 Response and Tolerance. *Journal of Integrative Plant Biology*, *50*(10), 1256-
776 1267.

777 Macías-Sámano, J., & Cibrían-Tovar, J. (1989). *Evaluación mediante fotografía*
778 *aérea infrarroja de la mortalidad de Abies religiosa en el parque Desierto de*
779 *los Leones.* IV Simposio Nacional sobre Parasitología forestal, México.

780 María L. España-Boquera, María L. España-Boquera, Omar Champo-Jiménez,
781 Omar Champo-Jiménez, María D. Uribe-Salas, & María D. Uribe-Salas.
782 (2022). Phenological variation and greening of the Monarch Butterfly
783 Biosphere Reserve (2000-2019). *Revista Chapingo serie ciencias forestales y*
784 *del ambiente*, *28*(2), 207-223.

785 Mateo-Bonmatí, E., Casanova-Sáez, R., Šimura, J., & Ljung, K. (2021). Broadening
786 the roles of UDP-glycosyltransferases in auxin homeostasis and plant
787 development. *New Phytologist*, *232*(2), 642-654.

Miller, P. R., de Lourdes de la Isla de Bauer, M., Quevedo-Nolasco, A., Abel Quevedo Nolasco, Nolasco, A. Q., & Tejeda, T. H. (1994). Comparison of ozone exposure characteristics in forested regions near Mexico City and Los Angeles. *Atmospheric Environment*, *28*(1), 141-148.

Molina, Velasco, Retama, & Zavala. (2019). Experience from Integrated Air Quality Management in the Mexico City Metropolitan Area and Singapore. *Atmosphere*, *10*(9), 512.

Moura, B. B., Paoletti, E., Badea, O., Ferrini, F., & Hoshika, Y. (2022). Visible Foliar Injury and Ecophysiological Responses to Ozone and Drought in Oak Seedlings. *Plants*, *11*(14), Article 14.

Müller-Starck, G., & Schubert, R. (Eds.). (2001). *Genetic Response of Forest Systems to Changing Environmental Conditions* (Vol. 70). Springer Netherlands.

Natali, L., Vangelisti, A., Guidi, L., Remorini, D., Cotrozzi, L., Lorenzini, G., Nali, C., Pellegrini, E., Trivellini, A., Vernieri, P., Landi, M., Cavallini, A., & Giordani, T. (2018). How Quercus ilex L. saplings face combined salt and ozone stress: A transcriptome analysis. *BMC Genomics*, *19*(1), 872.

Nunn, A. J., Weiser, G., Reiter, I. M., Häberle, K.-H., Grote, R., Havranek, W. M., & Matyssek, R. (2006). Testing the unifying theory of ozone sensitivity with mature trees of Fagus sylvatica and Picea abies. *Tree Physiology*, *26*(11), 1391-1403.

ONU, (2018). https://www.un.org/es/

Ortiz de Elguea-Culebras, G., Sánchez-Vioque, R., Berruga, M. I., Herraiz-Peñalver, D., & Santana-Méridas, O. (2017). Antifeedant effects of common terpenes from Mediterranean aromatic plants on Leptinotarsa decemlineata. *Journal of Soil Science and Plant Nutrition*, *ahead*.

Palomäki, V., Hassinen, A., Lemettinen, M., Oksanen, T., Helmisaari, H.-S., Holopainen, J., Kellomäki, S., Holopainen, T., A, L., & Holopainen, K. (1998). Open-top chamber fumigation system for exposure of field grown Pinus sylvestris to elevated carbon dioxide and ozone concentration. *Silva Fennica*, *32*.

Pan, Y., Xu, P., Zeng, X., Liu, X., Shang, Q., & Shang, Q.-L. (2019). Characterization of UDP-Glucuronosyltransferases and the Potential Contribution to Nicotine Tolerance in Myzus persicae. *International Journal of Molecular Sciences*, *20*(15), 3637.

Pellegrini, E., Cioni, P., Francini, A., Lorenzini, G., Nali, C., & Flamini, G. (2012). Volatiles Emission Patterns in Poplar Clones Varying in Response to Ozone. *Journal of chemical ecology*, *38*, 924-932.

Poland, J. A., & Rife, T. W. (2012). Genotyping-by-Sequencing for Plant Breeding and Genetics. *The Plant Genome*, *5*(3), plantgenome2012.05.0005.

Purcell, S., Neale, B., Todd-Brown, K., Thomas, L., Ferreira, M. A. R., Bender, D., Maller, J., Sklar, P., de Bakker, P. I. W., Daly, M. J., & Sham, P. C. (2007). PLINK: A Tool Set for Whole-Genome Association and Population-Based Linkage Analyses. *American Journal of Human Genetics*, *81*(3), 559-575.

832 Richards, C. L., Alonso, C., Becker, C., Bossdorf, O., Bucher, E., Colomé-Tatché,
833 M., Durka, W., Engelhardt, J., Gáspár, B., Gogol-Döring, A., Grosse, I., van
834 Gurp, T., Heer, K., Kronholm, I., Lampei, C., Latzel, V., Mirouze, M.,
835 Opgenoorth, L., Paun, O., … Verhoeven, K. J. F. (2017). Ecological plant
836 epigenetics: Evidence from model and non-model species, and the way
837 forward. *Ecology Letters*, *20*(12), 1576-1590.

838 Rivkin, L. R., Santangelo, J. S., Alberti, M., Aronson, M. F. J., de Keyzer, C. W.,
839 Diamond, S. E., Fortin, M.-J., Frazee, L. J., Gorton, A. J., Hendry, A. P., Liu,
840 Y., Losos, J. B., MacIvor, J. S., Ryan A. Martin, Martin, R., McDonnell, M. J.,
841 Miles, L. S., Munshi-South, J., Ness, R. W., … Johnson, M. T. J. (2019). A
842 roadmap for urban evolutionary ecology. *Evolutionary Applications*, *12*(3),
843 384-398.

844 Robinson, M. D., McCarthy, D. J., & Smyth, G. K. (2010). edgeR: A Bioconductor
845 package for differential expression analysis of digital gene expression data.
846 *Bioinformatics (Oxford, England)*, *26*(1), 139-140.

847 Sandermann, H., Wellburn, A. R., & Heath, R. L. (Eds.). (1997). *Forest Decline and*
848 *Ozone: A Comparison of Controlled Chamber and Field Experiments* (Vol.
849 127). Springer Berlin Heidelberg.

850 Sandoval, Z. E., Rojas, A., Guzmán, C., Carmona, L., Ponce, M., León, C., Loyola,
851 C., Vallejo, A., & Medina, A. (2005). *Técnicas Aplicadas al Estudio de la*
852 *Anatomía Vegetal.* (Vol. 38). Instituto de Biología, UNAM.

853 Santangelo, J. S., Rivkin, L. R., & Johnson, M. T. J. (2018). The evolution of city life.
854 *Proceedings of The Royal Society B: Biological Sciences*, *285*(1884),
855 20181529.

856 Schraudner, M., Moeder, W., Wiese, C., Camp, W. V., Inzé, D., Langebartels, C., &
857 Sandermann, H. (1998). Ozone-induced oxidative burst in the ozone
858 biomonitor plant, tobacco Bel W3. *The Plant Journal: For Cell and Molecular*
859 *Biology*, *16*(2), 235-245.

860 SEDEMA. (2018). *Calidad del aire en la Ciudad de México. Informe Anual*.

861 Seinfeld, J. H. (1989). Urban Air Pollution: State of the Science. *Science*, *243*(4892),
862 745-752.

863 Sethuraman, A. (2018). Estimating Genetic Relatedness in Admixed Populations. *G3*
864 *(Bethesda, Md.)*, *8*(10), 3203-3220. https://doi.org/10.1534/g3.118.200485

865 Srikant, T., & Drost, H.-G. (2021). How Stress Facilitates Phenotypic Innovation
866 Through Epigenetic Diversity. *Frontiers in Plant Science*, *11*, 606800.

867 Tammam, A., Badr, R., Abou-Zeid, H., Hassan, Y., & Bader, A. (2019). Nickel and
868 ozone stresses induce differential growth, antioxidant activity and mRNA
869 transcription in *Oryza sativa* cultivars. *Journal of Plant Interactions*, *14*(1), 87-
870 101.

871 Tausz, M., Grulke, N. E., & Wieser, G. (2007). Defense and avoidance of ozone
872 under global change. *Environmental Pollution*, *147*(3), 525-531.

873 Terrazas, T., & Bernal-Salazar, S. (2002). *Histological Symptoms of Air Pollution*
874 *Injury in Foliage, Bark, and Xylem of Abies religiosa in the Basin of Mexico*
875 (pp. 261-282).

876 Van Bel M., Proost S., Van Neste C., Deforce D., Van de Peer Y., Vandepoele K.
877 TRAPID: an efficient online tool for the functional and comparative analysis of de
878 novo RNA-Seq transcriptomes. *Genome Biol.* 2013; 14:R134.

879 Vickers, C. E., Possell, M., Cojocariu, C. I., Velikova, V. B., Laothawornkitkul, J.,
880 Ryan, A., Mullineaux, P. M., & Nicholas Hewitt, C. (2009). Isoprene synthesis
881 protects transgenic tobacco plants from oxidative stress. *Plant, Cell &*
882 *Environment*, *32*(5), 520-531.

883 Vollenweider, P., Ottiger, M., & Günthardt-Goerg, M. S. (2003). Validation of leaf
884 ozone symtoms in natural vegetation using microscopical methods.
885 *Environmental Pollution*, *124*, 101-118.

886 Waldeck, N., Burkey, K., Carter, T., Dickey, D., Song, Q., & Taliercio, E. (2017).
887 RNA-Seq study reveals genetic responses of diverse wild soybean
888 accessions to increased ozone levels. *BMC Genomics*, *18*(1), 498.

889 Xue Wang, Yuanfan Xu, H. Fan, N. Cui, Xiangnan Meng, Jiajing He, Nana Ran, &
890 Yang Yu. (2023). Research Progress of Plant Nucleotide-Binding Leucine-
891 Rich Repeat Protein. *Horticulturae*.

892 Zhang, L., Zhang, L., Xu, B., Xu, B., Wu, T., Wen, M., Fan, L., Feng, Z., & Paoletti,
893 E. (2017). Transcriptomic analysis of Pak Choi under acute ozone exposure
894 revealed regulatory mechanism against ozone stress. *BMC Plant Biology*,
895 *17*(1), 236-236.

Visual abstract:

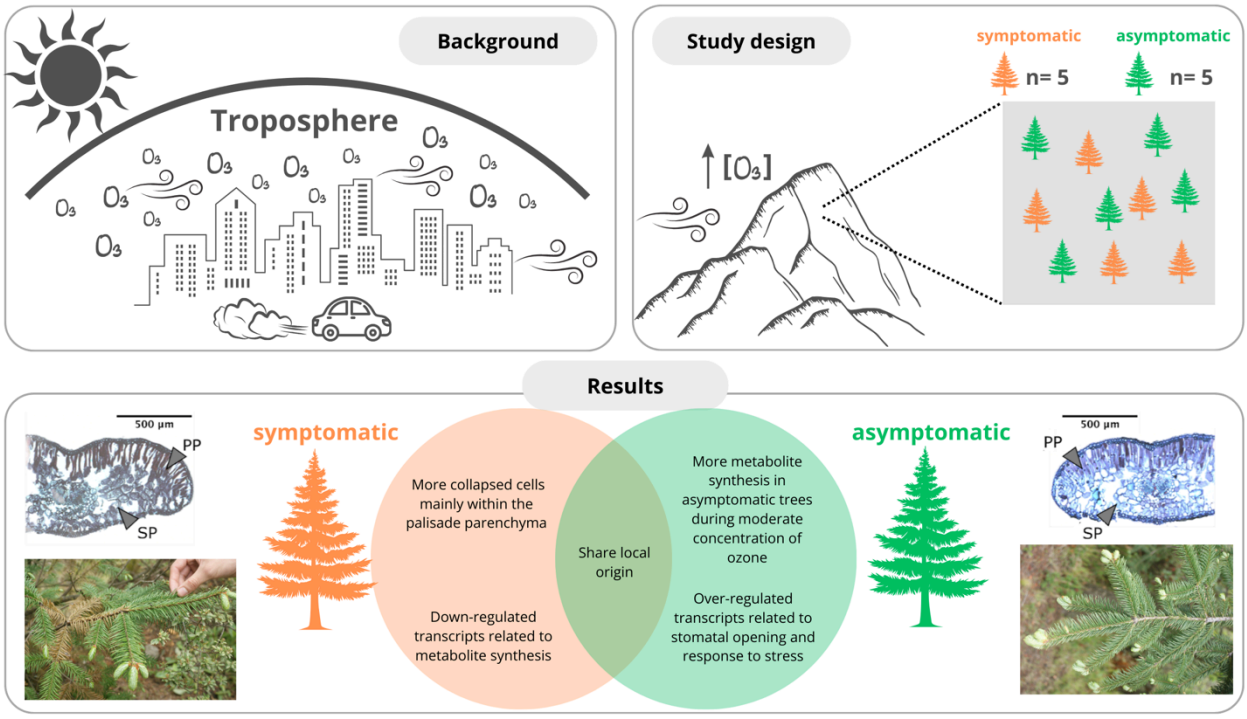

a)

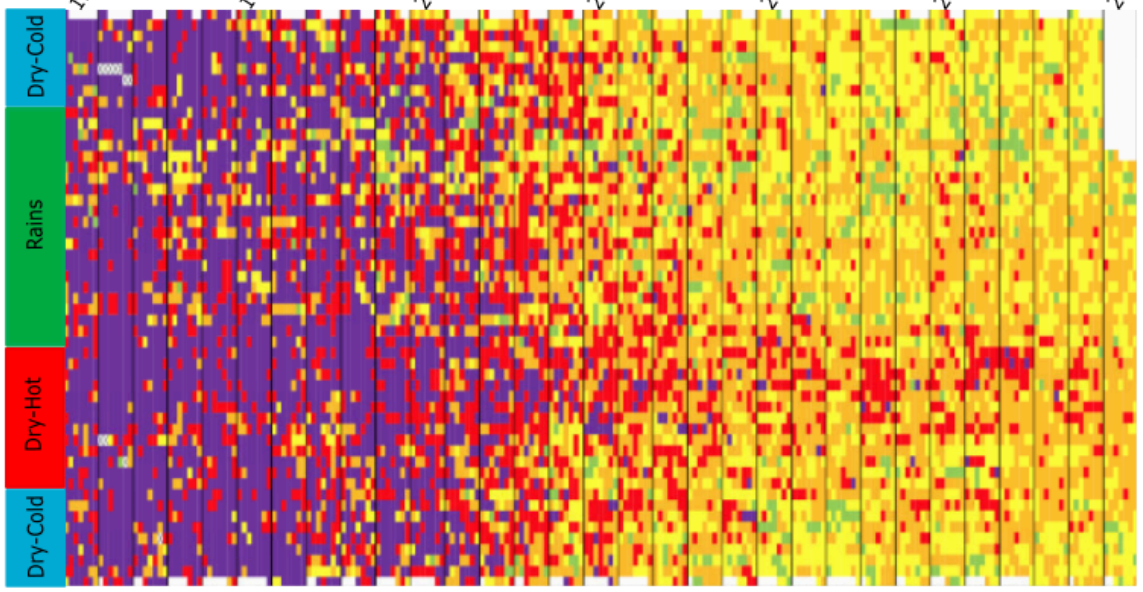

b)

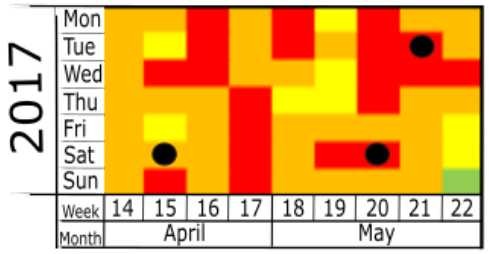

c)

Hour	15 April	13-14 May	17 May
13:00	70 ppb	105-96 ppb	132 ppb
14:00	81 ppb	109-94 ppb	158 ppb
15:00	87 ppb	125-95 ppb	170 ppb

d)

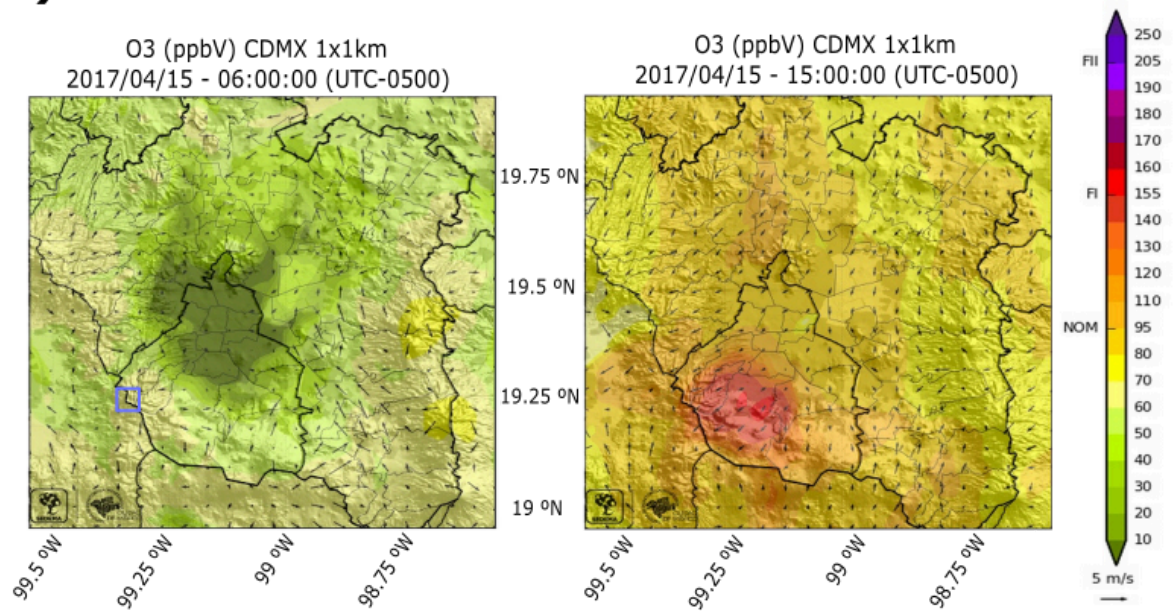

Figure 1 Change of O_3 concentration in the Mexico City (CDMX) metropolitan area since 1990 (a) Air quality is represented by colors: green, good (0-70ppb); yellow, regular (71-95ppb); orange, bad (96-154ppb); red, very bad (155-204ppb) and purple, extremely bad (> = 205). Modified of SEDEMA (2020) (b) average O_3 concentration during the study period (April and May, 2017). Black circles show collection days. (c) O_3 concentration as measured at the nearby station to the sampling site (PEDREGAL) during the sampling period. Modified of SEDEMA (2018) (d) wind direction and O_3 concentration in CDMX at 6:00 am (~ 50 ppb; left) and at 15:00 pm (~ 130 ppb; middle; see colorimetric scale at right) on a regular day between April and May. Blue boxes indicate the location of the study site. Arrow size indicates wind speed; vector at right (below colored bar) shows 5 m / s.

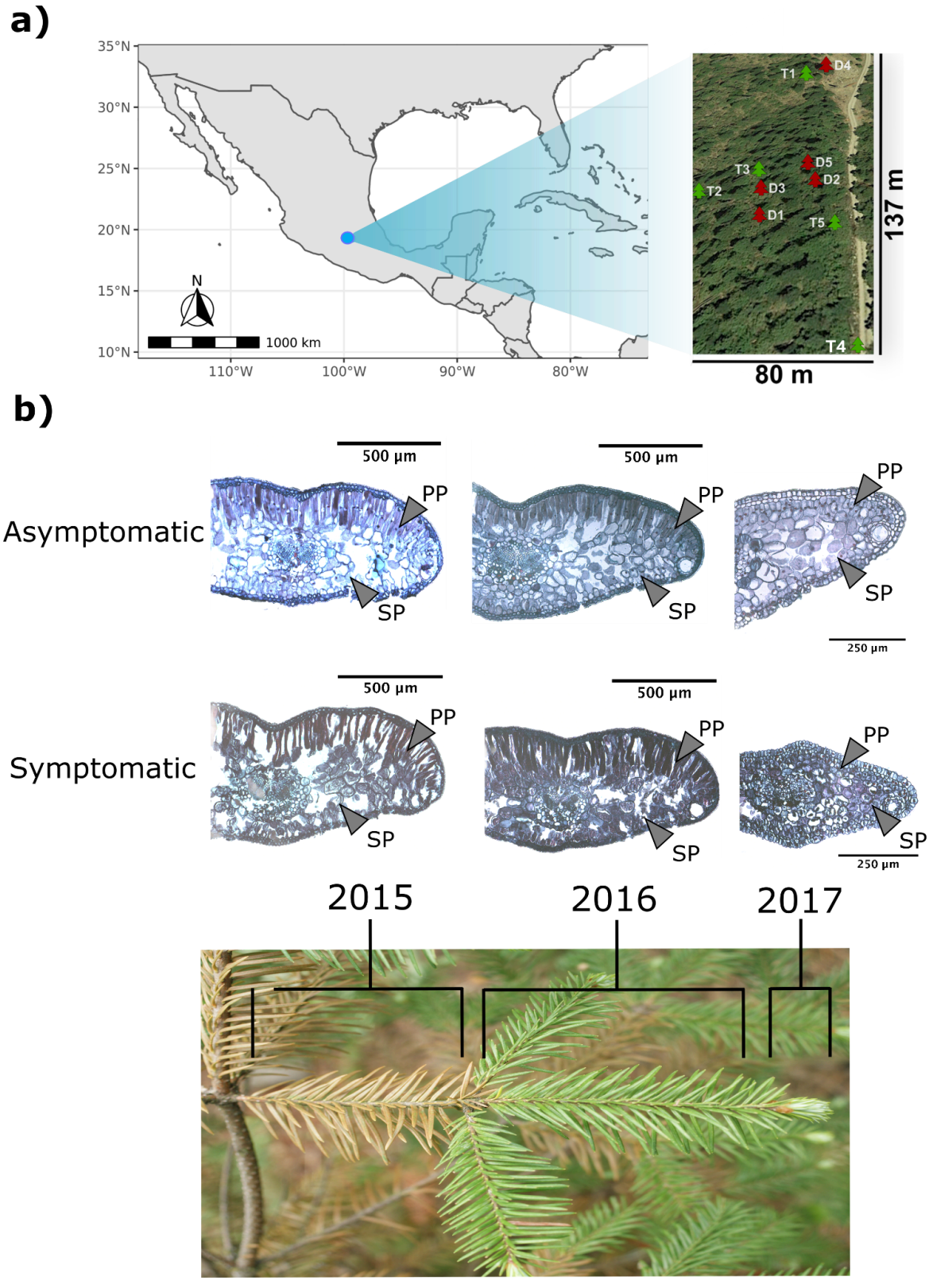
a)
35°N
30°N
25°N
20°N
15°N
10°N
110°W
100°W
90°W
80°W
N
1000 km
T1
D4
T3
D5
D2
T2
D3
D1
T5
T4
137 m
80 m
b)
Asymptomatic
Symptomatic
500 µm
PP
SP
250 µm
2015
2016
2017

Figure 2 Distribution of focus trees (asymptomatic in green, T1-5; symptomatic in red, D1-5) within the study site, and location of the study site within Mexico City metropolitan area and Mexico (a) Transverse histological sections of needles from asymptomatic (left) and symptomatic (right) sacred fir individuals (*Abies religiosa*) for three growth periods (2015, 2016, 2017) (b) All bars = 10μm. PP, palisade parenchyma; SP, spongy parenchyma.

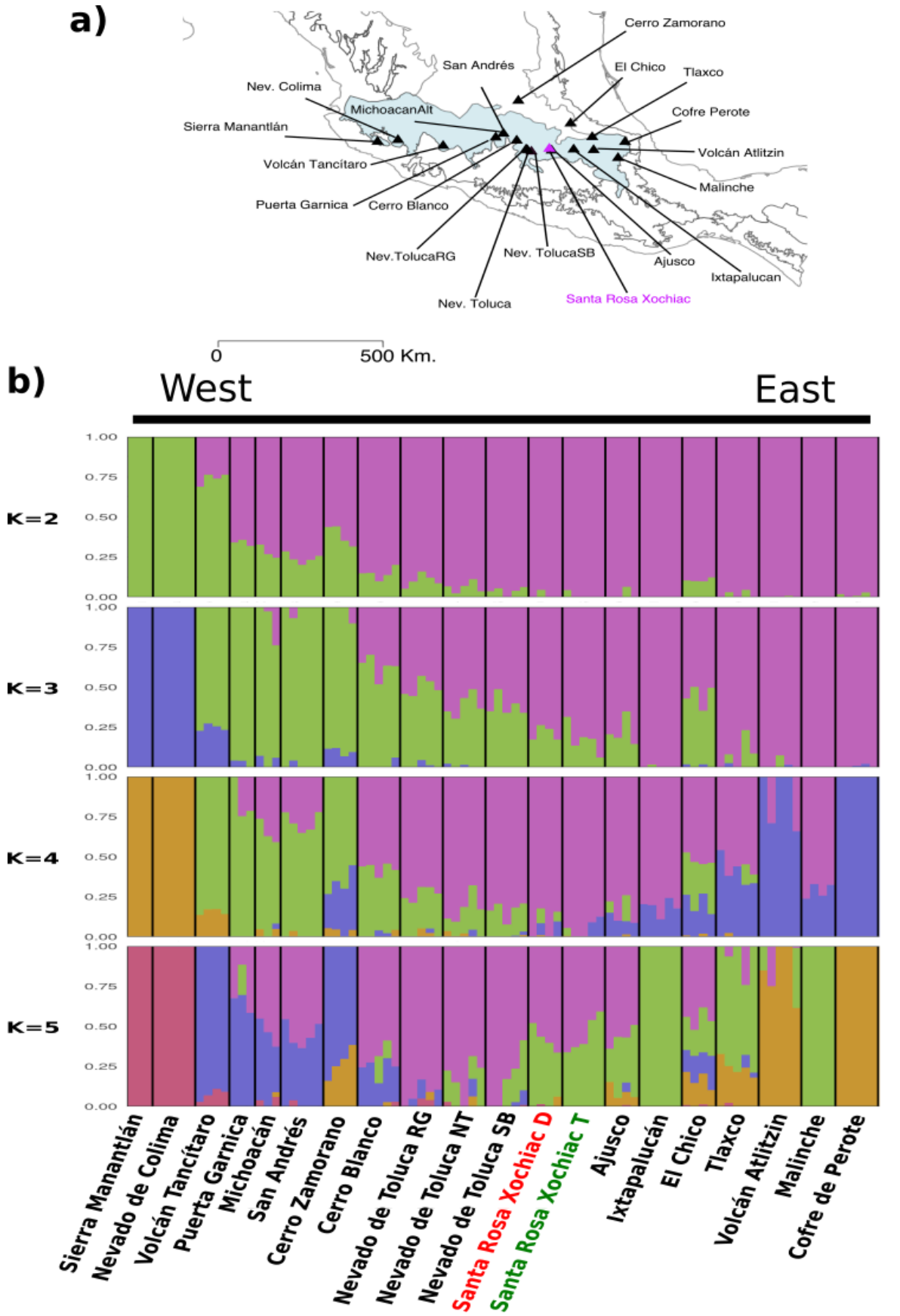
a)
Cerro Zamorano
San Andrés
El Chico
Tlaxco
Nev. Colima
MichoacanAlt
Cofre Perote
Sierra Manantlán
Volcán Atlitzin
Volcán Tancítaro
Malinche
Puerta Garnica
Cerro Blanco
Nev.TolucaRG
Nev. ToluccaSB
Ajusco
Ixtapalucan
Nev. Toluca
Santa Rosa Xochiac
0
500 Km.
b)
West
East
K=2
K=3
K=4
K=5
1.00
0.75
0.50
0.25
0.00
Sierra Manantlán
Nevado de Colima
Volcán Tancítaro
Puerta Garnica
Michoacán
San Andrés
Cerro Zamorano
Cerro Blanco
Nevado de Toluca RG
Nevado de Toluca NT
Nevado de Toluca SB
Santa Rosa Xochiac D
Santa Rosa Xochiac T
Ajusco
Ixtapalucán
El Chico
Tlaxco
Volcán Atlitzin
Malinche
Cofre de Perote

Figure 3. Assignment of studied individuals to the species genetic clusters based on admixture results (derived from 1,550 SNPs). Symptomatic trees indicated in red below figure; asymptomatic trees in green. Plots are shown for k = 2 to k = 5, all of which denote identical cluster assignments for both types of trees. Individuals (n= 88) are shown as vertical bars colored in proportion to their estimated ancestry for each cluster. Black lines separate populations listed from West to East along the species distribution.

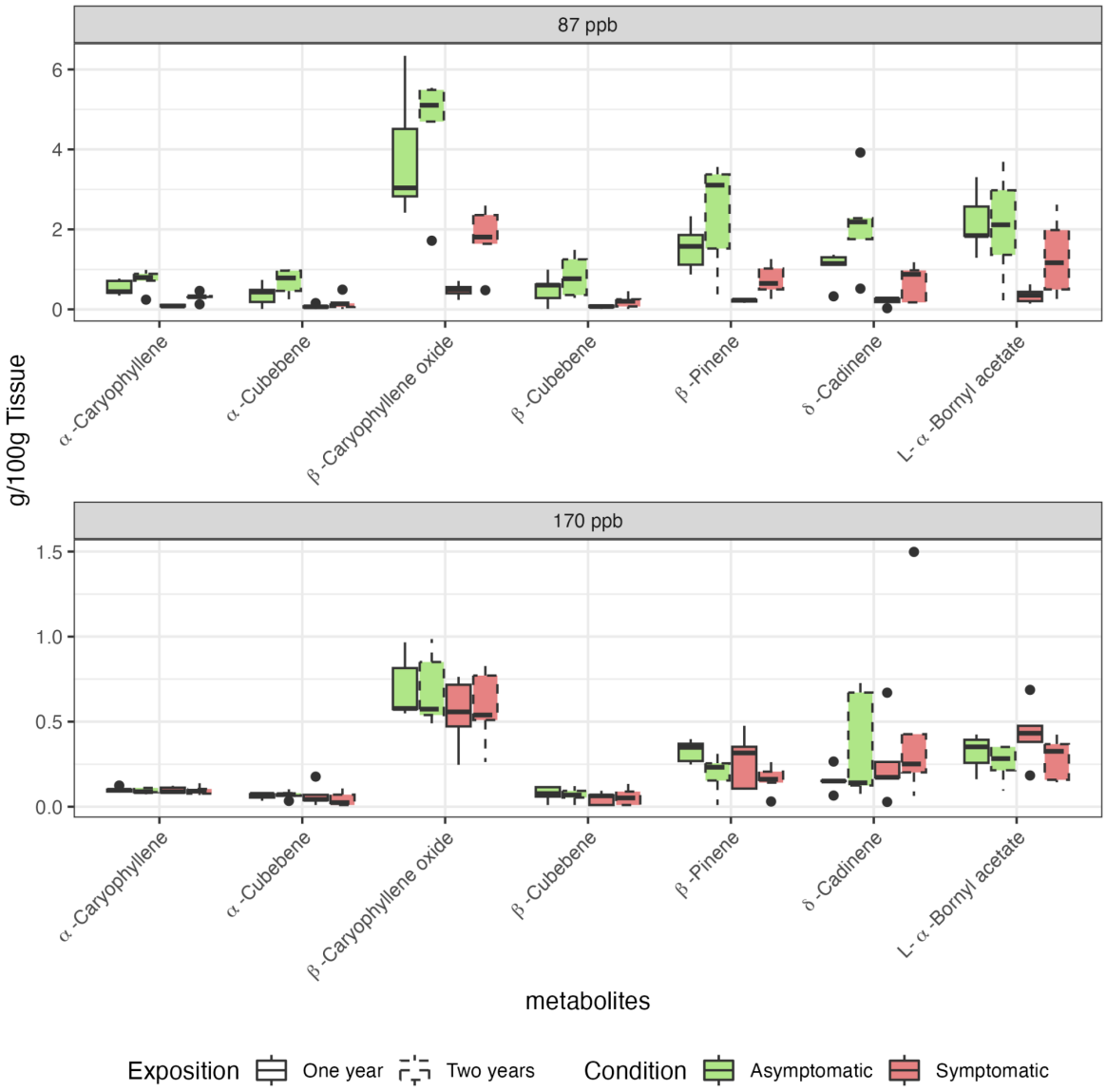

Figure 4 Relative sesquiterpene concentrations (mg / 100g dry weight) in needles from symptomatic (red) and asymptomatic (green) sacred fir (*Abies religiosa*) individuals during two periods with contrasting O_3 concentration (87ppb and 170 ppb). Measures taken from one- (continuous line) and two-year old (dashed line) needles. Bars show variability in comparison to the IQR. See table S4 to consult the statistical analyzes of interactions.

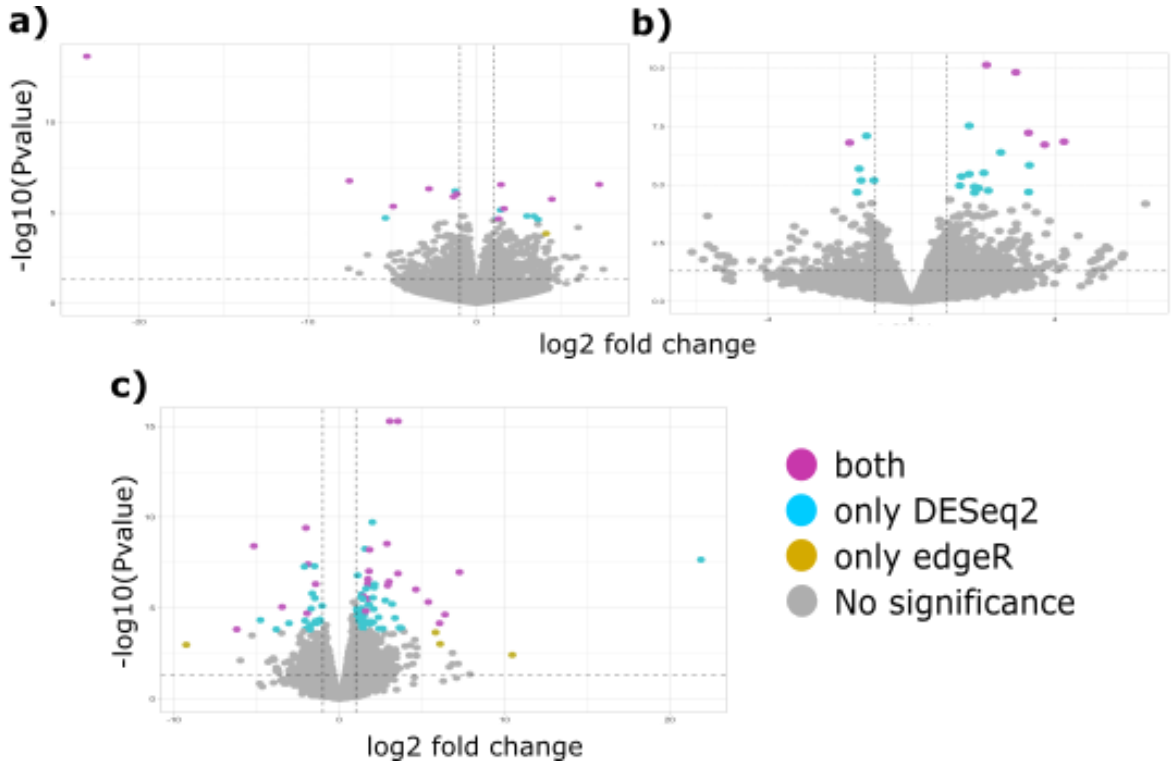

Figure 5 Differential Expression Analysis of RNA transcripts with two methods (DESeq2 in blue; edgeR in yellow; retained transcripts were those detected by both methods, in purple; $p < 0.005$). Volcano plots for asymptomatic vs. symptomatic trees during the high O_3 period (a); high vs. moderate O_3 concentration periods for symptomatic individuals (b); and high vs moderate O_3 concentration periods for asymptomatic trees (c). Differentially expressed transcripts were selected with thresholds of fold change > 2 (represented by two dotted black vertical lines) and $p < 0.005$ (represented by dotted black horizontal lines).

Supplementary Images

(a)

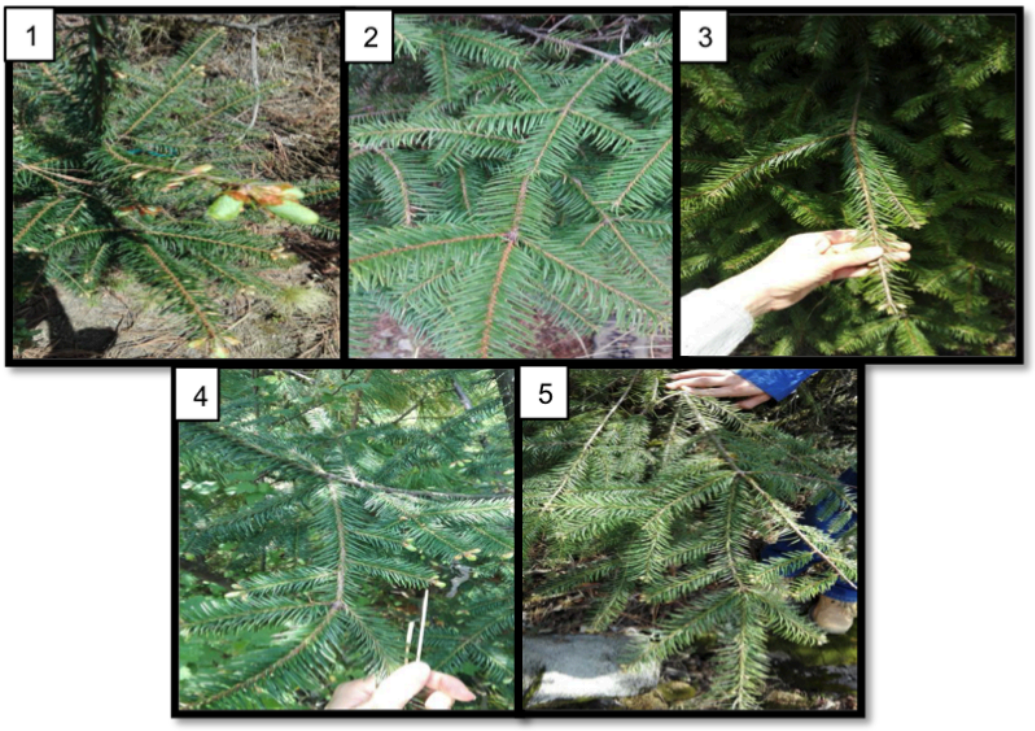

(b)

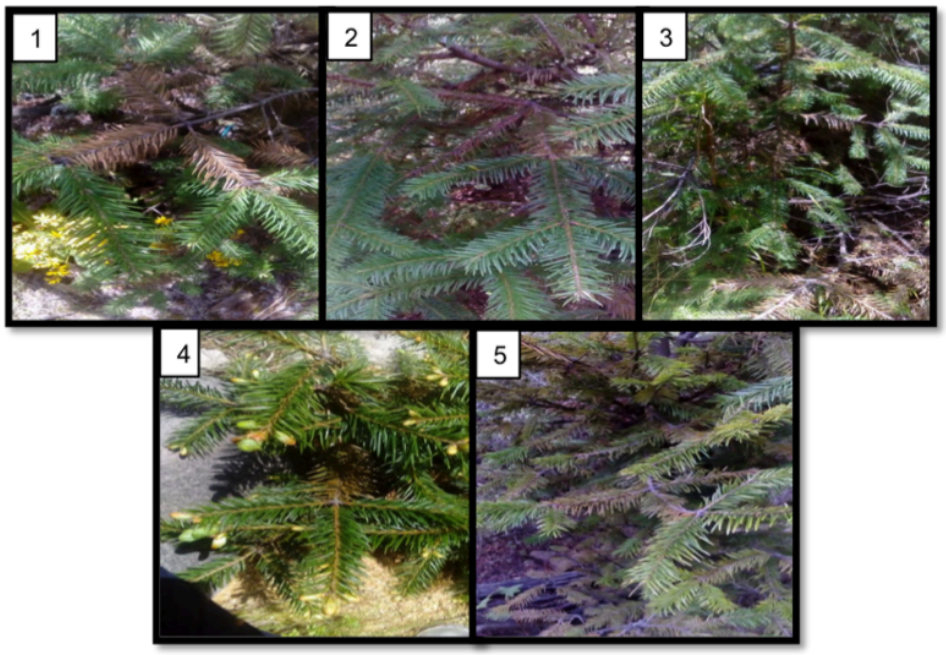

Figure S1 Photographs of the branches for each sampled sacred fir tree. **(a)** asymptomatic trees **(b)** symptomatic trees.

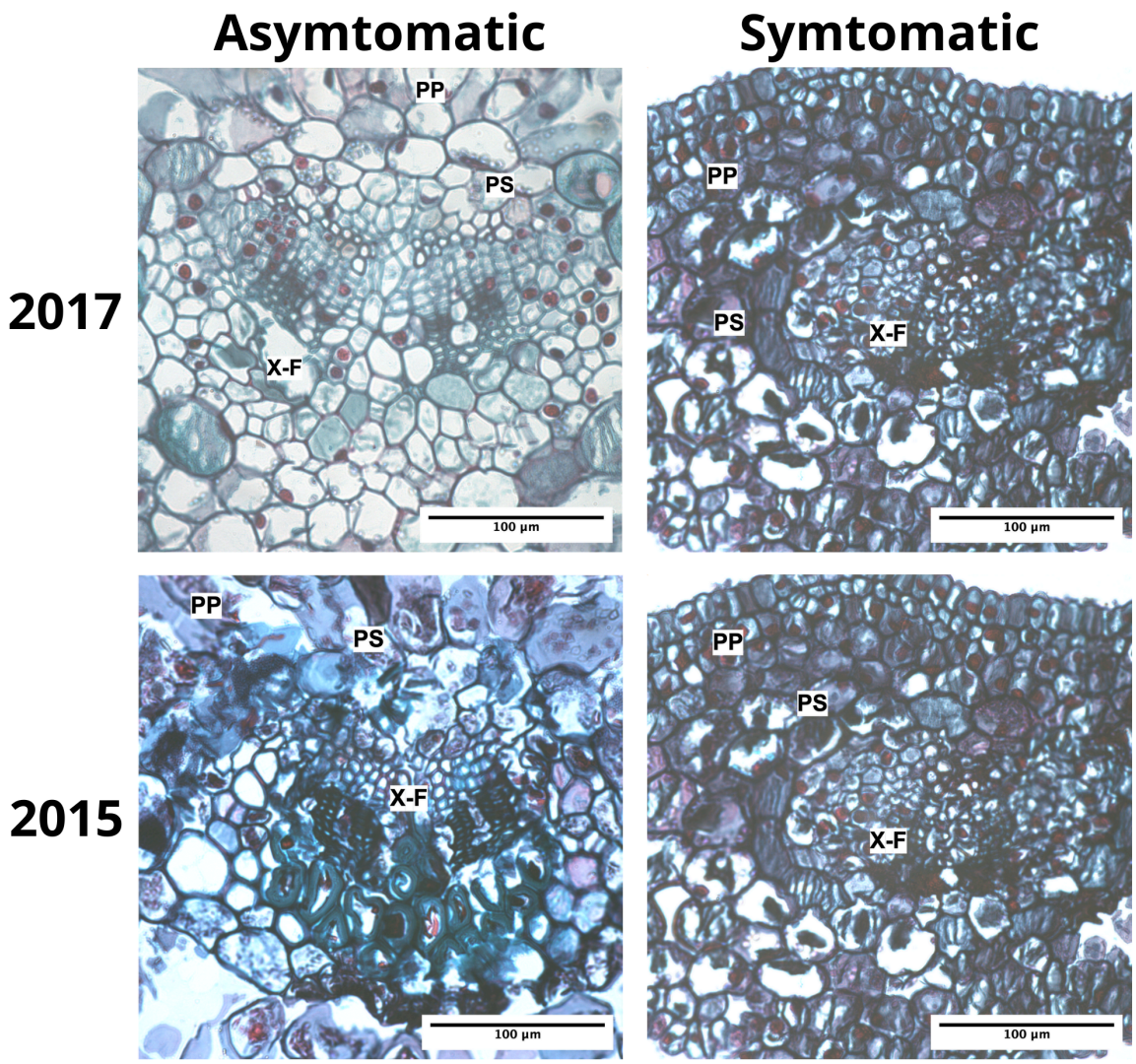

Figure S2 Histological sections of needles from asymptomatic (left) and symptomatic (right) sacred fir (*Abies religiosa*) individuals from two growing seasons (2017 top; 2015 bottom). All bars = 10µm. PP, palisade parenchyma; SP, spongy parenchyma; X-P, xylem and phloem.

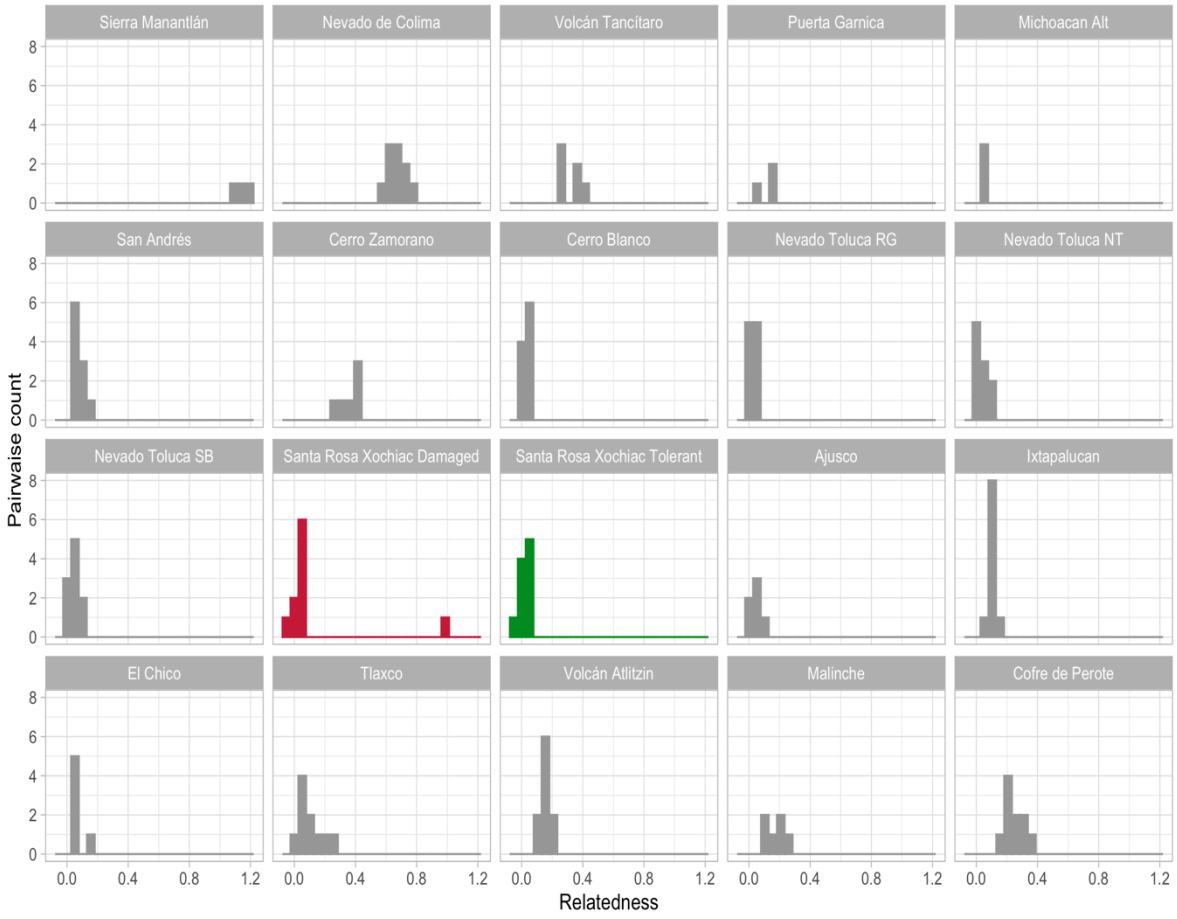

Figure S3 Relatedness between sacred fir (*Abies religiosa*) individuals used for genetic assignment analyses. Asymptomatic individuals from study sites in green, symptomatic trees in red.

TABLES

Table S1 Differentially expressed transcripts in symptomatic vs asymptomatic sacred fir (*Abies religiosa*)

Contig ID	**Log_2 fold change[a]**	**Query length, nts**	**Score[b] / Max query cover in the 1st 5 hits, %**	**Annotation**	**Notes**
AB_000588_T.1	7.257	707	L / 40	Hypothetical protein KI387_017072, partial [*Taxus chinensis*]	The only hit returned by the ncbi Blastx
AB_045531_T.1	4.450	1192	M / 68	Hypothetical protein	Mostly bacterial hits
AB_015092_T.1	1.614	1944	H / 89	*Nuclear fusion defective 4-like, Nodulin-like*	*Nuclear fusion defective 4* in *A. thaliana* is involved in response to salt stress (Sottosanto et al. 2007).
AB_036475_T.1	1.437	650	H / 78	*Chitinase* class VII / II / IV / or EP3-like / 4 / 5	Chitinases are involved in responses to various abiotic and biotic stresses. An acidic chitinase is **over-regulated after ozone exposure** in tobacco (Ernst et al. 1992)
AB_018867_T.1	1.302	409	L / 37	Unknown [*Picea sitchensis*]	Four hits in 2 unknown proteins of *P. sitchensis* (Could be conifer-specific protein)
AB_029334_T.1	-1.187	2594	H / 72	*Probable L-type lectin-domain containing receptor kinase S.5*	L-type lectin receptor kinases are involved in defense response to bacteria and oomycetes (Bouwmeester and Govers 2009).
AB_029013_T.1	-1.371	1214	VL / 21	Hypothetical protein	Three hits in two different OFRs

AB_035458_T.1 AB_038616_T.1	-2.8306 - 4.951	928 752	H / 99 H / 88	*Leucine-rich repeat (LRR) receptor-like serine/threonine protein kinase*	A large family of LRR receptor-like kinases (RLK) participate in all aspects of plant development, in response to abiotic stresses, in defense processes and in plant-microbe interactions. Loss of the LRR-RLK GHR1 **resulted in O3 sensitivity** in *A. thaliana*, likely mediated by the associated disruption of stomatal function (Sierla et al. 2018).
AB_027319_T.1	-7.549	895	L / 39	Tetratricopeptide repeat (TPR)-like / patatin-like phospholipase domain protein / oidium resistance required protein 1/ TOM1-like protein 2	Members of TPR protein superfamily includes ones with potential to interact with Hsp90/Hsp70 as co-chaperones in nucleus and cytoplasm, thus participating in response to biotic stresses; RNA binding proteins involved in mRNA edition in plastid and mitochondria, are involved in plant development. Patatin-like phospholipase domain proteins involved in plant development, synthesis of secondary metabolites, cell death, defense responses, response to abiotic stresses (Lebeda et al. 2014).

AB_038562_T.1	-23.104	951	No hit	No hit	No significant similarity either in BLASTn search in NCBI nr database, neither in congenie.

[a] Positive value: up regulated in symptomatic trees; Negative value: down regulated in symptomatic trees;
[b] H: high (>200); M: medium (80-200); L: low (50-80); VL: very low (40-50).

Table S2 Differentially expressed transcripts in symptomatic sacred fir trees during high vs moderate O_3 concentration periods.

ID Locus	Log_2 fold change[a]	Query length, nts	Score[b] / Max query cover in the 1st 5 hits, %	Annotation	Notes
AB_002157_T.1	4.255	609	VL / 30	Hypothetical protein [*Acinetobacter baumannii*]	NCBI BLASTn returns five hits of mRNA sequences of *Picea glauca* with 81.49% to 87.93% identity
AB_028063_T.1	3.717	1034	No hit	No hit	
AB_029211_T.1	3.265	1193	H / 44 (H / 76)	No Apical Meristem, (NAC) transcription factor (Unannotated protein [*Picea sitchensis*])	Members of the huge family of NAC transcription factors are involved in many aspects of plant development, defense response to bacteria and other organisms, response to water deprivation and to abscisic acid, secondary metabolic processes. ANAC013, ANAC016, ANAC017, ANAC053 and ANAC078 regulate oxidative stress in *A. thaliana* (De Clercq et al. 2013).
AB_023740_T.1	2.911	1320	H / 62	Xyloglucan endotrans glucosylase (XET) /hydrolase; Glycosyl hydrolase family 16	XET enzymes participate in cell wall remodeling, thus modulating its expansion and strength. The contig covers complete XET CDS. Expression of XET coding gene XTR9 **increased in response to O_3** (Zhang et al. 2017).

AB_015079_T.1	2.094	1291	M / 24	Linker histone H1	Linker (H1) histones are the most variable histones; H1.3 variant of *A. thaliana* is involved in adaptive responses to abiotic stress (Rutowicz et al. 2015).
AB_008838_T.1	-1.7	1312	H / 89	UDP-glucosyl transferase (UGT) 7-deoxyloganetin glucosyltransferase	The enzymes of the UGT family act on a variety of substrates and participates in many metabolic processes, including flavonol (e.g. UGT78D1/At1g30530), tetrapyrrole (e.g UGT85A1/AT1G22400) or terpenoid (e.g. UGT89B1/ AT1G73880) biosynthesis. Some UGTs involved in response to abiotic and biotic stresses (Rehman et al. 2018). Transcription of UGT78D2/At5g17050 gene was **decreased after O_3 exposure** for 2 days (Booker et al. 2012).

[a] Positive value: up regulated during high O_3 concentration periods; Negative value: down regulated during high O_3 concentration periods;
[b] H: high (>200); M: medium (80-200); L: low (50-80); VL: very low (40-50).

Table S3 Differentially expressed transcripts in asymptomatic sacred fir trees during high vs. moderate O_3 concentration periods**.**

ID Locus	Log_2 fold change[a]	Query length, nts	Score[b] / Max query cover in the 1st 5 hits, %	Annotation	Notes
AB_010244_T.1	7.274	2007	H / 59	Metal tolerance protein (MTP) 5, 11 Cation diffusion facilitator (CDF) efflux family proteín	Plant MTPs from CDF family are involved in enhancing resistance to heavy metal tolerance
AB_022453_T.1	6.398	613	M / 56	Pathogenesis-related (PR) thaumatin family protein	PR thaumatin family proteins are involved in defense response, response to fungus, to osmotic stress, to water deprivation, to wounding, regulation of metabolism and plant development (e.g. AT4G36010 and AT1G20030 in *A. thaliana*).
AB_040533_T.1	6.07	561	H / 90	Disease resistance-responsive dirigent-like protein	Many dirigent-like proteins are involved in defense response; some in response to wounding, cell wall biogenesis and metabolic processes.
AB_025629_T.1	5.388	1582	H, M / 88	LRR and NB-ARC domain disease resistance protein; disease resistance protein RPP13,	NB-ARC domain disease resistance (R) proteins in plants are involved in pathogen recognition and subsequent activation of innate immune responses. Besides, Glyma12g01420 was **upregulated in response to elevated ozone** in Glycine max (Leisner et al.

				RPM1, RGA2, RGA4	2014).
AB_022256_T.1	4.635	1436	H / 82 --	S-adenosyl methionine (SAM) synthase	Small family of plant S-adenosylmethionine synthases, or methionine adenosyltransferase (MAT) produces SAM from methionine and ATP. Methyl group of SAM can be transferred to a variety of molecules that includes nucleic acids, proteins, lipids and secondary metabolites. Therefore, the methylation rates for a variety of substrates affects multiple aspects of plant fitness. Besides, in plants SAM is a precursor of ethylene and polyamines. Histone and DNA methylation is highly important for the regulation of gene expression (Sekula et al. 2020).
AB_013716_T.1	3.549	1989	H / 74	3-ketoacyl (oxoacyl)-CoA synthase	Members of the 3-ketoacyl-CoA synthase family are involved in the biosynthesis of very long chain fatty acids (VLCFA), therefore, in cuticle development and wax and suberin synthesis. They also have an important role in response to cold, to light stimulus, to osmotic stress and to wounding
AB_043005_T.1	3.549	1193	M / 63	B-box-type Zinc finger and CCT domain protein CONSTANS-LIKE (COL)	COL transcription factors are involved in regulation of plant growth and development, control of flowering time and responses to stresses (Khatun et al. 2021).
AB_000610_T.1	3.054	1461	H / 68	beta-1,3-glucanase, or glucan endo-1,3-beta-glucosidase	Beta-1,3-glucanases degrade plant callose and components of plant, fungi and bacteria cell walls, therefore, are involved in defense response. Some of them are also involved in

					response to cold, heat and wounding.
AB_021997_T.1	2.999	2144	H / 81	Isocitrate lyase/ Phosphoenol pyruvate phosphomut ase	Isocitrate lyase is a glyoxylate cycle enzyme; it is involved in plant salt tolerance (Yuenyong et al. 2019).
AB_002147_T.1	2.926	1211	H / 82	Peroxidase 72 class III peroxidase	*A. thaliana* Peroxidase 72 (AT5G66390) is involved in lignin biosynthesis and in response to oxidative stress; many class III peroxidases are located in cell wall and involved in cell wall modification; some may play a role in generating H_2O_2 during defense response. **Near-ambient concentrations of ozone can induce ascorbate peroxidase** APX1 gene expression in *A. thaliana* and tobacco (Kubo et al. 1995, Wang et al. 1999). At least part of the induction of heat shock proteins during light stress in Arabidopsis is mediated by H_2O_2 that is scavenged by APX1.
AB_000596_T.1	2.883	475	No hit	No hit	
AB_013152_T.1	1.832	1494	H / 65	Carboxyleste rase 15; alpha/beta hydrolase fold	Carboxylesterases hydrolyze esters of short-chain fatty acids and involved in metabolism of jasmonic acid and salicylic acid and in systemic acquired resistance. They belong to the larger alpha/beta hydrolase fold superfamily of enzymes.
AB_028624_T.1	1.798	967	H / 40	Early nodulin-like (ENODL) with cupredoxin/ plastocyanin domain	Cupredoxins contain type I copper centers and are involved in inter-molecular electron transfer reactions. ENODLs extracellular proteins are anchored in the plasma membrane.

					AtENODL1 (AT5G53870) transcript is up-regulated in leaves of *A. thaliana* subjected to a combination of drought and heat stress. AtENODL2 (AT4G27520) is involved on responses to water deprivation, abscisic acid, salt stress, light and temperature stimuli (Rizhsky et al. 2004).
AB_031334_T.1	1.736	752	M / 40	Zinc finger Ran-binding domain-containing protein 2; RNA-binding protein c17h9.04c; UPF0481 protein	Mammalian zinc finger Ran-binding domain-containing protein 2 is an RNA-binding protein involved in alternative splicing.
AB_015079_T.1	1.73	1291	M / 24	Histone H1	Linker (H1) histones are the most variable histones; H1.3 variant of *A. thaliana* is involved in adaptive responses to abiotic stress (Rutowicz et al. 2015).
AB_039330_T.1	1.601	974	L (M) / 25	Hypothetical protein (plants), Set1 complex component ash2	The Set1 complex specifically methylates Lys-4 of histone H3 (H3K4). H3K4me is an epigenetic modification involved in the **regulation (induction) of gene expression.**
AB_013119_T.1	1.429	465	No hit		Two Picea NCBI BLASTn hits suggest that it could be conifer-specific polyA RNA.
AB_018867_T.1	-1.431	409	L / 37	Unknown protein [*Picea sitchensis* only]	Could represent a conifer-specific protein
AB_000811_T.1	-1.949	1592	H / 61	Flavonol synthase	Some 2OG-Fe(II) oxygenases (as AT5G24530

				2OG-Fe(II) oxygenase GA2ox9, GA2ox10	in *A. thaliana*) participates in flavonoid biosynthesis; therefore, they may be involved in response to salicylic acid and defense response to bacteria, oomycetes and fungus. A homology to GA2ox9 that contribute to cold stress tolerance and involved in response to water deprivation and wounding (Lange et al. 2020), is also revealed.
AB_029470_T.1 AB_008960_T.1	-3.459 -5.169	1182 1226	H / 69 H / 80	(Iso)eugenol synthase 1, isoflavone reductase, propenylphenol synthase 1 NmrA-like protein NAD(P)H-binding NAD dependent epimerase/dehydratase family	The inferred proteins possess similarity to several classes of enzymes with Rossman fold. Among them are the isoflavone reductases involved in response to oxidative stress and to wounding, as well as the propenylphenol synthases involved in synthesis of phenylpropanoid compounds, propenyl-phenols (Wibe et al. 1997), presumed to serve mainly in defense against herbivores and parasites.
AB_000071_T.1	-6.206	1408	H / 60	Ferritin, desiccation-related protein PCC13-62	Arabidopsis ferritins are essential to protect cells against oxidative damage (Ravet et al. 2009).

[a] Positive value: up regulated during high O_3 concentration periods; Negative value: down regulated during high O_3 concentration periods;
[b] H: high (>200); M: medium (80-200); L: low (50-80); VL: very low (40-50).

Table S4 Wilcoxon Test. Interactions between Condition (asymptomatic or symptomatic), Needle age (2015 or 2016) and Period (high or moderate).

	Period moderate 87 ppb		**Period high**170 ppb	
	Metabolite	**Sig.**	**Metabolite**	**Sig.**
Condition Asymptomatic - Symptomatic	α-caryophyllene	0.0004871**	α-caryophyllene	N.S.
	α-Cubebene	0.007197*	α-Cubebene	N.S.
	β-Caryophyllene	0.0001299**	β-Caryophyllene	N.S.
	β-Cubebene	0.004525*	β-Cubebene	N.S.
	β-Pinene	0.0004871**	β-Pinene	N.S.
	δ-Cadinene	0.0007253**	δ-Cadinene	N.S.
	Bornyl acetate	0.0115*	Bornyl acetate	N.S.
Needle age one-year and two-years exposition	α-caryophyllene	N.S.	α-caryophyllene	N.S.
	α-Cubebene	N.S.	α-Cubebene	N.S.
	β-Caryophyllene	N.S.	β-Caryophyllene	N.S.
	β-Cubebene	N.S.	β-Cubebene	N.S.
	β-Pinene	N.S.	β-Pinene	N.S.
	δ-Cadinene	N.S.	δ-Cadinene	N.S.
	Bornyl acetate	N.S.	Bornyl acetate	N.S.

	Metabolite	**Sig.**
Period 87ppb - 170 ppb	α-caryophyllene	0.001953*
	α-Cubebene	0.003906*
	β-Caryophyllene	0.001953*
	β-Cubebene	0.003906*
	β-Pinene	0.001953*
	δ-Cadinene	0.005859*
	Bornyl acetate	0.001953*

(***) Significant at the 0.0001 probability level. (**) Significant at the 0.001 probability level. (*) Significant at the 0.05 probability level. (.) Significant at the 0.1 probability level. (ns) nonsignificant.

Table S5 Number of genes mapped for each sample.

Tree condition	O3 concentration period	ID sample	Number of genes identified as expressed**	Number of genes with no reads mapped*
Asymptomatic	high	Asymptomatic 1	37,601	0
		Asymptomatic 2	33,200	4,401
		Asymptomatic 3	34,182	3,419
		Asymptomatic 4	34,840	2,761
		Asymptomatic 5	33,366	4,235
	moderate	Asymptomatic 1	35,460	2,141
		Asymptomatic 2	34,256	3,345
		Asymptomatic 4	35,031	2,570
symptomatic	high	Symptomatic 1	34,048	3,553
		Symptomatic 2	33,983	3,618
		Symptomatic 3	34,060	3,541
		Symptomatic 4	33,663	3,938
		Symptomatic 5	33,981	3,620
	moderate	Symptomatic 1	35,738	1,863
		Symptomatic 2	35,020	2,581
		Symptomatic 5	34,293	3,308

***Number of genes with no reads mapped**: refers to genes without any reads mapped to the reference transcriptome of *A. balsamea,* considering the total number of mapped genes.

** **Number of genes identified as expressed:** refers to genes with reads mapped to the reference transcriptome of *A. balsamea.*

Table S6 RNA-seq data per sample.

Sample	Total reads	Mapped	Mapped %	Properly paired	Properly paired %	Singletons	Singletons %
Asymptomatic 1	26628465	25110645	94.30%	23207744	87.79%	190570	0.72%
Asymptomatic 2	29394389	27421473	93.29%	25506062	87.47%	216864	0.74%
Asymptomatic 3	28885822	26935913	93.25%	25005412	87.24%	206331	0.72%
Asymptomatic 4	27148620	24890979	91.68%	23160294	85.90%	190051	0.70%
Asymptomatic 5	25402180	22810050	89.80%	21279266	84.36%	153044	0.61%
Asymptomatic 1	86373044	80384008	93.07%	74602376	87.09%	601512	0.70%
Asymptomatic 2	39848295	36957834	92.75%	34301814	86.78%	271419	0.69%
Asymptomatic 4	30581813	28117524	91.94%	26128276	86.06%	188559	0.62%
Symptomatic 1	29917209	26626122	89%	24575346	82.81%	204199	0.69%
Symptomatic 2	20519755	19680381	95.91%	18198494	89.39%	124258	0.61%
Symptomatic 3	34920801	33514452	95.97%	30677044	88.59%	257139	0.74%
Symptomatic 4	33932229	30786857	90.76%	28520838	84.73%	245596	0.73%
Symptomatic 5	34662281	32472479	93.68%	30328610	88.12%	230530	0.67%
Symptomatic 1	29755812	25145836	84.51%	23338336	79.07%	219234	0.74%
Symptomatic 2	32034433	29891742	93.31%	27696704	87.09%	228013	0.72%
Symptomatic 5	39785361	35702980	89.74%	32688214	82.84%	330867	0.84%

Supplementary references

Booker F, Burkey K, Morgan P, Fiscus E, Jones A (2012) Minimal influence of G-protein null mutations on ozone-induced changes in gene expression, foliar injury, gas exchange and peroxidase activity in Arabidopsis thaliana L.: Minimal influence of G-proteins on ozone responses. Plant Cell Environ 35:668–681.

Bouwmeester K, Govers F (2009) Arabidopsis L-type lectin receptor kinases: phylogeny, classification, and expression profiles. J Exp Bot 60:4383–4396.

De Clercq I, Vermeirssen V, Van Aken O, Vandepoele K, Murcha MW, Law SR, Inzé A, Ng S, Ivanova A, Rombaut D, van de Cotte B, Jaspers P, Van de Peer Y, Kangasjärvi J, Whelan J, Van Breusegem F (2013) The Membrane-Bound NAC Transcription Factor ANAC013 Functions in Mitochondrial Retrograde Regulation of the Oxidative Stress Response in Arabidopsis. Plant Cell 25:3472–3490.

Ernst D, Schraudner M, Langebartels C, Sandermann H (1992) Ozone-induced changes of mRNA levels of β-1,3-glucanase, chitinase and 'pathogenesis-related' protein 1b in tobacco plants. Plant Mol Biol 20:673–682.

Khatun K, Debnath S, Robin AHK, Wai AH, Nath UK, Lee D-J, Kim C-K, Chung M-Y (2021) Genome-wide identification, genomic organization, and expression profiling of the CONSTANS-like (COL) gene family in petunia under multiple stresses. BMC Genomics 22:727.

Kubo A, Saji H, Tanaka K, Kondo N (1995) Expression of arabidopsis cytosolic ascorbate peroxidase gene in response to ozone or sulfur dioxide. Plant Mol Biol 29:479–489.

Lange T, Krämer C, Pimenta Lange MJ (2020) The Class III Gibberellin 2-Oxidases AtGA2ox9 and AtGA2ox10 Contribute to Cold Stress Tolerance and Fertility. Plant Physiol 184:478–486.

Lebeda A, Mieslerová B, Petřivalský M, Luhová L, Špundová M, Sedlářová M, Nožková-Hlaváčková V, Pink DAC (2014) Resistance mechanisms of wild tomato germplasm to infection of Oidium neolycopersici. Eur J Plant Pathol 138:569–596.

Leisner CP, Ming R, Ainsworth EA (2014) Distinct transcriptional profiles of ozone stress in soybean (Glycine max) flowers and pods. :13.

Ravet K, Touraine B, Boucherez J, Briat J-F, Gaymard F, Cellier F (2009) Ferritins control interaction between iron homeostasis and oxidative stress in Arabidopsis. Plant J 57:400–412.

Rehman HM, Nawaz MA, Shah ZH, Ludwig-Müller J, Chung G, Ahmad MQ, Yang SH, Lee SI (2018) Comparative genomic and transcriptomic analyses of Family-1 UDP glycosyltransferase in three Brassica species and Arabidopsis indicates stress-responsive regulation. Sci Rep 8:1875.

Rizhsky L, Liang H, Shuman J, Shulaev V, Davletova S, Mittler R (2004) When defense pathways collide. The response of Arabidopsis to a combination of drought and heat stress. Plant Physiol 134:1683–1696.

Rutowicz K, Puzio M, Halibart-Puzio J, Lirski M, Kroteń MA, Kotliński M, Kniżewski Ł, Lange B, Muszewska A, Śniegowska-Świerk K, Kościelniak J, Iwanicka-Nowicka R, Żmuda K, Buza K, Janowiak F, Jõesaar I, Laskowska-Kaszub K, Fogtman A, Zielenkiewicz P, Tiuryn J, Kollist H, Siedlecki P, Ginalski K, Świeżewski S, Koblowska M, Archacki R, Wilczyński B, Rapacz M, Jerzmanowski A (2015) A specialized histone H1 variant is

required for adaptive responses to complex abiotic stress and related DNA methylation in Arabidopsis. Plant Physiol:pp.00493.2015.

Sekula B, Ruszkowski M, Dauter Z (2020) S-adenosylmethionine synthases in plants: Structural characterization of type I and II isoenzymes from Arabidopsis thaliana and Medicago truncatula. Int J Biol Macromol 151:554–565.

Sierla M, Hõrak H, Overmyer K, Waszczak C, Yarmolinsky D, Maierhofer T, Vainonen JP, Salojärvi J, Denessiouk K, Laanemets K, Tõldsepp K, Vahisalu T, Gauthier A, Puukko T, Paulin L, Auvinen P, Geiger D, Hedrich R, Kollist H, Kangasjärvi J (2018) The Receptor-like Pseudokinase GHR1 Is Required for Stomatal Closure. Plant Cell 30:2813–2837.

Sottosanto JB, Saranga Y, Blumwald E (2007) Impact of AtNHX1, a vacuolar Na+/H+ antiporter, upon gene expression during short- and long-term salt stress in Arabidopsis thaliana. BMC Plant Biol 7:18.

Wang J, Zhang H, Allen RD (1999) Overexpression of an Arabidopsis Peroxisomal Ascorbate Peroxidase Gene in Tobacco Increases Protection Against Oxidative Stressl. :8.

Wibe A, Borg-Karlson A-K, Norin T, Mustaparta H (1997) Identification of plant volatiles activating single receptor neurons in the pine weevil (Hylobius abietis). J Comp Physiol A 180:585–595.

Yuenyong W, Sirikantaramas S, Qu L-J, Buaboocha T (2019) Isocitrate lyase plays important roles in plant salt tolerance. BMC Plant Biol 19:472.

Zhang L, Xu B, Wu T, Wen M, Fan L, Feng Z, Paoletti E (2017) Transcriptomic analysis of Pak Choi under acute ozone exposure revealed regulatory mechanism against ozone stress. BMC Plant Biol 17:236.